ENVIRONMENTAL AND ANTHROPOGENIC INFLUENCES DURING THE 20TH CENTURY IN SCOTT BAY SAN JACINTO ESTUARY, HOUSTON, TEXAS

A Thesis

By

LISA MADELEINE BARØ HILL

Submitted to the Office of Graduate and Professional Studies of
Texas A&M University
in partial fulfillment of the requirements for the degree of

MASTER OF SCIENCE

Chair of Committee,	Timothy Dellapenna
Committee Members,	Niall Slowey
	Wesley Highfield
Head of Department,	Kyeong Park

August 2020

Major Subject: Marine Resource Management

TABLE OF CONTENTS

FIGURES AND TABLES

ABSTRACT

In the past century the San Jacinto Estuary (SJE), including the Houston Ship Channel (HSC) and its surrounding area, has experienced a significant increase in industrialization and urbanization. As a result of industrialization, sediments accumulating in the bay are contaminated with pollutants. In the past century, this area has also experienced up to 3 m of land subsidence due to anthropogenic groundwater removal for growing urbanization.

Other influences on the watershed and bay are storm associated floods, like that of Hurricane Harvey which hit the Texas coast on August 25, 2017 causing record rain fall in the Houston and Harris County areas resulting in severe flooding. A storm of this magnitude has the possibility to significantly disturb the sediment column to release any previously buried pollutants and to flood the nearby EPA Superfund sites, adding to the toxins in the water column with the potential for further impact to the area.

In two parts, this study reconstructed the history of an environmental change from riverine to estuarine dominated system in the San Jacinto Estuary by the identification of benthic foraminifera ecology shift, and historic storm events through several sediment cores taken pre-Hurricane Harvey. The pre-Harvey core analysis indicated a few clear signals correlating to historical Hurricane storm events and the building of the San Jacinto Dam. A closer look at the contaminants found in the pre-Harvey cores indicated an increased abundance of

“stressed” benthic foraminifera individuals correlating with the prominent Hg peaks identified in core SB1. The benthic foraminifera record also indicated there was a significant change in the environment indicated by a change from no saline/ brackish, therefore riverine environment, specific species below 100cm, down core, to the estuarine environment species, like that of *Ammonia beccari*, becoming the dominant species in the Scott Bay and lower SJE region.

Then in the second part, Hurricane Harvey influenced the estuary system by causing massive amounts of freshwater to flood the environment causing erosion and a redistribution of previously buried contaminants. The pre-Harvey core samples indicated Hg concentrations being lower than that of the Post-Harvey Hg concentrations due to the flux of freshwater from the floods eroding the river beds and redistributing previously buried Hg concentrations, as well as the benthic foraminifera record showing that the flux of freshwater from SJR and Buffalo Bayou flooding caused a decrease in saline specific species abundance closer to the HSC bed.

This study proved evident how highly influenced the lower San Jacinto Estuary system is influenced, not only by the anthropogenic activities near by, but the significant storm events that come through the area.

ACKNOWLEDGEMENTS

I would like to thank my committee members Dr. Timothy Dellapenna, Dr. Niall Slowey and Dr. Wesley Highfield for seeing me through the last tough months with their guidance and support.

A special thank you to the lab of Laboratory for Environmental and Oceanographic Research and Dr. Kathy Schwehr and Dr. Peter Santchi for allowing me access to their hot lab equipment for my lead 210 processing and counting and Dr. Peter Santchi for his further advise on my calculation methods.

I am tremendously grateful to the Coastal Geology Laboratory for their invaluable contributions in the collection of all the core samples used in this research, especially Lindsay Critides for really being the driving force behind the field process, and Dr. Pete Van Hengstum for the use of his wonderful microscope collection and guidance with the benthic foraminifera processing.

CONTRIBUTORS AND FUNDING SOURCES

Contributors

This work was supported by a thesis (or) dissertation committee consisting of Professor Dr. Timothy Dellapenna and committee members Dr. Niall Slowey of the Department of Oceanography and Dr. Wesley Highfield of the Department of Marine Resource Management.

The core samples collected in Chapter I and II was done in part by Lindsay Critides along with various student workers of the Coastal Geology Labs. The GC/MS results were provided by the GERG team in College Station.

All other work conducted for the thesis (or) dissertation was completed by the student independently.

Funding Sources

There are no outside funding contributions to acknowledge related to the research and compilation of this document.

NOMENCLATURE

Hg	Mercury
^{210}Pb	Radioactive Lead isotope
^{238}U	Radioactive Uranium isotope
^{222}Rn	Radon isotope 222
CWA	Clean Water Act (1972)
EOE	Estimated Oil Equivalent
EPA	Environmental Protection Agency
FEMA	Federal Emergency Management Agency
GC/MS	Gas-Chromatography/ Mass Spectrometry
GERG	Texas A&M University Geochemistry Environmental Research Group
HSC	Houston Ship Channel
IPCC	Intergovernmental Panel on Climate Change
MeHg	Methylmercury
NPL	EPA National Priorities List
PAHs	Polycyclic aromatic hydrocarbons
PCBs	Polychlorinated biphenyl
SJE	San Jacinto Estuary
TCEQ	Texas Commission on Environmental Quality
USACE	U.S. Army Corps of Engineers

CHAPTER I: INTRODUCTION

Scott Bay, adjacent to the Houston Ship Channel (HSC), is a semi-isolated embayment within the San Jacinto Estuary (SJE), and is located in the upper reaches of Galveston Bay (Figure 1). The Houston Ship Channel (HSC) extends 13 km up along the lower reach of the SJE to where it meets the Buffalo Bayou, 5 km upstream of Scott Bay, and up into the heart of the Port of Houston. The Port of Houston encompasses the largest manufacturing and refining center for petrochemicals in the US and the second largest complex in the world (Port of Houston, 2018). A significant increase in industrialization and urbanization over the past century has resulted, in some cases, severe alterations to Galveston Bay's estuarine systems (White et al., 1993; Santschi et al., 2001; USGS, 2002; Byun et al. 2004; Ravens et al., 2009; Al Mukaimi et al., 2018a, and Al Mukaimi et al., 2018b).

Subsidence caused by groundwater (Coplin and Galloway, 1999) and, oil and gas extraction has resulted in: natural habitat loss (**Figure 1**) (White et al., 1993), a higher frequency of flooding (USGS, 2002) and enhanced accumulation of contaminated sediments (Morse et al., 1993; Wen et al., 1999; Santschi et al., 2001; Al Mukaimi et al., 2018a). The area around the SJE and the HSC has also experienced up to 3 m of land subsidence in the past 80 years, resulting in the accommodation space for up to 3 m of highly contaminated sediment within the SJE (Al Mukiaimi et al., 2018a and b), including highly elevated mercury (Hg)

concentrations that are up to 100 times the background concentration (Morse et al., 1993; Wen et al., 1999; Santschi et al., 2001; Al Mukaimi et al., 2018a).

Previous studies of the HSC area have exposed some of the environmental effects from industrial activity (Santschi et al., 2001; Yeager et al., 2010). Living in a close proximity, 3.2 km, of the HSC results in a 56% higher risk of contracting leukemia (University of Texas, 2007). Harmon et al. (2003) found a homogenous distribution of trace metals, at around 200 ng g-1 concentration, in the surface sediments of the HSC, which is almost four times the concentrations found in other estuary systems. Al Mukaimi et al. (2016) concluded (prior to Hurricane Harvey) that the area around Scott Bay may not see a full Hg recovery before 2044, but only if the status quo is maintained and no major storms occur.

On August 25th Hurricane Harvey made landfall near Rockport, TX as a Category 4 hurricane. Over the next 5 days Hurricane Harvey stalled over the Texas coast depositing over 12cm of rain per hour (MetStat). This record rainfall

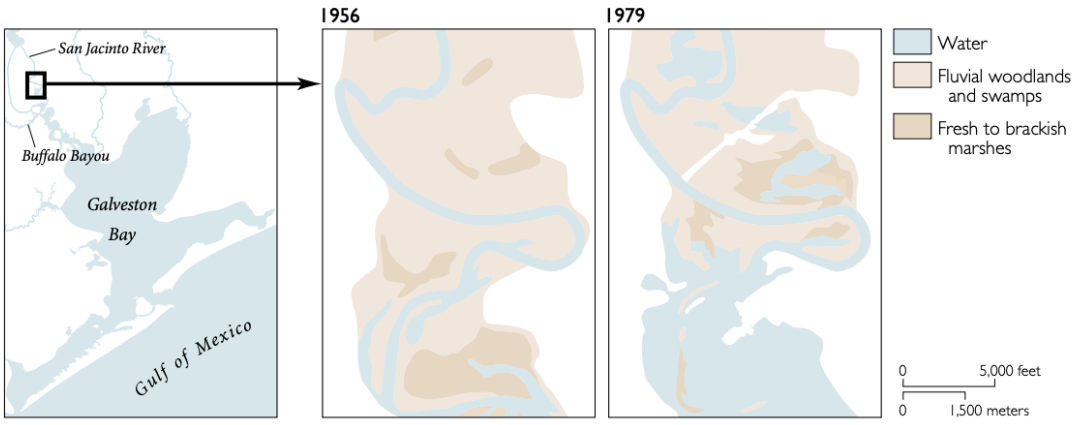

Figure 1: Wetland loss of lower San Jacinto River due to inundation from local land subsidence (White et al., 1993).

resulted in a 1000 year record flooding event of Houston bayous and water ways, all of which drained into the San Jacinto Estuary (SJE), with its main tributaries being Buffalo Bayou and the San Jacinto River. Buffalo Bayou flooded for 44 days due to the controlled water releases from the Addicts and Barker Reservoirs, whereas the San Jacinto River (SJR) only flooded for 7 days due to the release of storm waters from Lake Houston reservoir (Du et al., 2019). As a result, the three reservoirs, with the combination of 73% contribution from the Buffalo Bayou and the San Jacinto River natural discharge, resulted in the release of 11.1×10^9 m^3 amount of freshwater flowing into Galveston Bay, a volume equivalent to 3.6 times the volume of the entire bay (Du et al., 2019). Du et al. (2019) document that the current velocity at the Morgan Point tidal gauge, at the mouth of the SJE, was in excess of 3 m s^{-1}, and the currents were comparable throughout the lower SJE and Buffalo Bayou. Where the bay bottom is constituted primarily of soft estuarine muds, these currents would have been sufficiently high to cause extensive bed erosion. Contained within the SJE are two EPA Superfund Sites which were flooded, one of which is on the National Priorities List. Numerous pollution studies in the area have been conducted (Morse et al., 1993; Ravichandran et al., 1995; Wen et al., 1999; Santchi et al., 1995, 2001; Harmon et al., 2003; Yeager et al., 2007; Howell et al., 2011) which are described in this study. The respective drainage basins of Buffalo Bayou and San Jacinto River contain additional, flooded Superfund Sites as well as the Petrochemical complex in Houston which

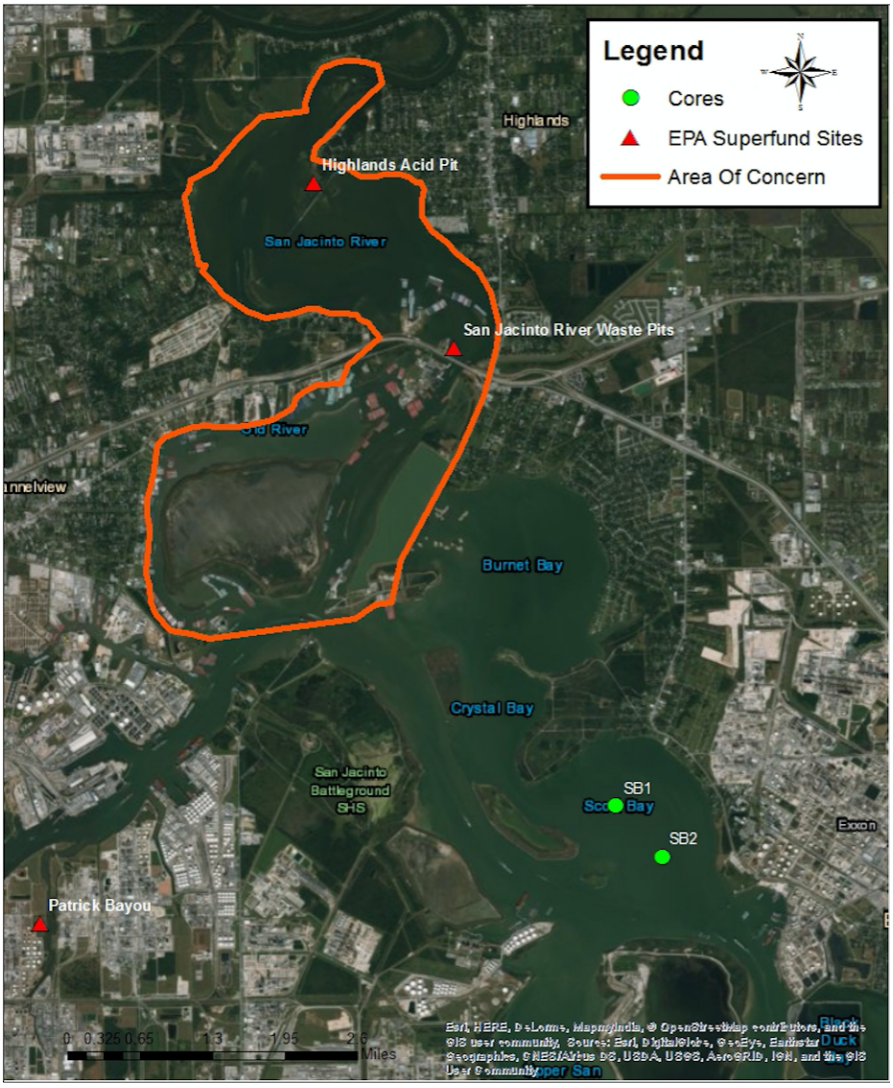

Figure 2: Designated EPA Superfund sites and Area of Concern, with core locations of SB1 and SB2 in Scott Bay. Created in ArcGIS based off of EPA Superfund location map, TCEQ, and USACE.

provides a significant potential source of new contaminants to enter the system and be dispersed into the bay.

This study builds upon the results of previous work conducted by Al Mukaimi et al. (2016), with the addition of two vibracores from Scott Bay collected in 2016, to analyze the environmental influences of the past century. Several post-

Hurricane Harvey (2017) push cores were acquired as comparison from the same area. The two 2016 vibracores from Scott Bay were analyzed for water and organic matter content, grain size, mercury (Hg) content, lead (^{210}Pb) activity, and benthic foraminifera assemblages (**Figure 2**). Certain target layers within the two cores were subsampled for Gas-chromatography analysis (GC/MS) and sent to the Geochemistry Environmental Research Group (GERG) at Texas A&M University main campus (College Station). The post-Harvey (2017) cores were only analyzed for Hg content in the identifiable "storm layer" and pre-Harvey, mud layer for comparisons and through these analyses, the mass accumulation rate of Mercury into Scott Bay was determined. There are two chapters to this thesis, Chapter I: The Environmental and Pollution Geologic Record from Past Century in Scott Bay, addresses the following hypotheses:

H1: *Historic events like that of the building of San Jacinto Dam and large hurricanes/storms will be indicated by a decrease in sand or clay deposits, respectively*.

H2: *The increase in urbanization around Scott Bay will indicate an increase in mercury (Hg) concentration and therefore cause the benthic foraminifera to show indication of stress.*

H3: *With the addition of subsidence and sea concentration rise, then the benthic foraminifera record should show a change from a riverine environment*

with no species diversity to a predominant species common in estuarine/saline environments.

Chapter II: Hurricane Harvey's Effect on Erosion and Deposition in San Jacinto Estuary, addresses the following hypotheses:

H1: *The amount of Hg deposited in SJE, as a result of the erosion of the river bed during Hurricane Harvey, is less than the amount of Hg previously buried within the SJE Hurricane Harvey flood layer.*

H2: *The benthic foraminifera estuarine specific species, as a result from the flux of freshwater from San Jacinto river and Buffalo Bayou flooding during Hurricane Harvey, will show a decrease in abundance closer to river mouth.*

1.1: Background

Study Site Characteristics

The study focuses on Scott Bay, a semi enclosed estuarine embayment, adjacent to the Houston Ship Channel (HSC) (**Figure 2**). The HSC in the study area, is 4 km downstream of the confluence of Buffalo Bayou and the SJE. Until the mid-1970s Scott Bay was partially isolated from the main-stem of the SJE both to the north and west due to the presence of an isthmus and island. However, in the mid-1970s this protection was largely removed due to the expansion of the HSC and by continual elevated subsidence from the 1950s. Following the last major expansion of the HSC (circa 2000), dredge spoil islands, or barriers, were re-established and now partially shelter Scott Bay from the HSC.

The Port of Houston encompasses the largest manufacturing and refining center for petrochemicals in the US and the second largest complex in the world (Port of Houston, 2018). Included in this is the ExxonMobil Baytown refinery, the second largest petrochemical complex in the world, which occupies the entire eastern side of Scott Bay, and is set back from the shoreline by only 150-200 m, separated by a row of bay front homes. The complex extends nearly 4 km to the east of Scott Bay. Its location allows direct access to the HSC, which has been further facilitated by dredging and expansion of the HSC for high-tonnage vessel access to the refineries of the greater Port Houston area.

A large increase in urban development can be correlated to an increase in pollution in the form of urban runoff, human waste, reduced air quality due to

atmospheric fallout (Santchi et al., 1995, 2001), an increase in the contamination of sediment (Morse et al., 1993; Wen et al., 1999; Santschi et al., 2001; Al Mukaimi et al., 2018a), and the presence of trash and other pollutants in the environment (e.g. hydrocarbons, pesticides, fertilizer, PCBs and other, since banned environmental polluting chemicals) (Ravichandran et al., 1995; Wen et al., 1999; Harmon et al., 2003; Yeager et al., 2007; Howell et al., 2011; Al Mukaimi et al., 2018a). Howell et al. (2011) conducted a study of the HSC to examine contaminant patterns of Poly-Chlorinated Biphenyl (PCBs) in the sediment. Whereas Harmon et al. (2003) found a homogeneous distribution of approximately 200 ng g^{-1} of trace metals in the surface sediments in the HSC, which is almost four times the amount that has been found in other locations.

Previous studies of the HSC area have addressed some of the environmental impacts from industrial activities (Santschi et al., 2001; Yeager et al., 2010). The air quality proximal to the HSC petrochemical complex is sufficiently poor, according to Linder et al. (2008), that the neighborhoods by the Bay Shores area has a 70% increased cumulative cancer risk from point source pollution, about 7 times greater than the Harris county average. It has also been found that overall proximity to the ship channel has also been proven to have a higher risk for childhood leukemia, where living within 3.2km of the HSC has a 56% higher risk than those living 16km away (Whitworth et al., 2008).

Howell (2011) conducted a study of the HSC to examine contaminant patterns of PCBs, the study identified a possible source of such contaminants in

the bottom sediments of the channel where the same pollutant concentration was also found buried in Scott Bay. Harmon et al. (2003) found a homogenous distribution of trace metals at around 200 ng g^{-1}, in the surface sediments of the HSC, which is almost four times the concentrations found in other estuary systems in the US. Families living in this area are therefore potentially affected by not only the air quality but also the water quality.

In order to support the petrochemical industries and urban growth in the lower drainage basin, elevated groundwater removal has occurred in the area. The groundwater drawdown has resulted in a reduction in the geostatic pressure, and this has resulted in the collapse of the clay lattice structure within the aquifer. Consequently, marshes and other low-lying areas subsided and became open bay, increasing the overall flood risk to the area (Coplin and Galloway, 1999, and Al Mukaimi et al., 2018b). The land proximal to the SJE has, as a result, subsided by around 3 cm per year over the past 100 years (Al Mukaimi, et al. 2018a; Al Mukaimi, et al. 2018b). The forward impact of eustatic sea concentration change is expected to have a sea concentration rise by 1 m, or more, over the next century (IPCC, 2013). This therefore may add an extra 1cm y^{-1} to the local, relative sea concentration rise. For these estuarine systems to be maintained in their current form, an equilibrium of sediment supply and accommodation space formation (relative sea concentration rise) must exist (Nichols, 1989; Al Mukaimi, et al. 2018b). As a result, the frequency and intensity of local flooding may be

expected to cause: increased damage to the urban infrastructure, further increase in environmental pollutant runoff and wetland loss (Kennish, 2002).

In 1972, the Environmental Protection Agency (EPA) enacted the Clean Water Act (CWA). Under the CWA water quality standards for surface water contaminants were implemented making it unlawful to discharge point source pollution into navigable waters without a permit. In addition, the CWA introduced regulations to protect aquatic ecosystems in order to protect human health. However, by this time, the study area, had already experienced an extensive and detrimental impact to its ecosystem due to rapid industrial growth exasperated by the human modification of the Lower San Jacinto River system following expansion of the HSC (USGS, 2002; Al Mukaimi, et al. 2018a; Al Mukaimi, et al. 2018b). **Figure 2**, depicts the highly polluted area that the EPA has highlighted as an "Area of Concern." Within this area are two Superfund Sites: the San Jacinto paper mill disposal waste pits and the Highlands Acid pit, which are part of the EPA National Priorities List (NPL). Both are upstream of the San Jacinto River, and in close proximity to the core locations in Scott Bay, as well as Patrick Bayou, a highly polluted waterway, in upstream Buffalo Bayou.

Mercury (Hg)

Mercury (Hg) is naturally found in the earth's biogeochemical cycles and within the earth's crust. Hg can be released into the atmosphere by anthropogenic emissions as a result of fossil fuel combustion and from other, Hg containing, consumer products. Power plants that burn coal in the USA, for

example, account for around 42% of all anthropogenic mercury emissions (EPA,1997).

Hg that reaches the ecosystem combines with carbon to form the organic methylmercury (MeHg) compound. If exposed to marine aquatic life the compound can travel up trophic concentrations to birds and mammals, such as eagles and otters, through aquatic life like fish and benthic invertebrate organisms which are even more susceptible to such pollutants. As Hg travels up the food chain it becomes increasingly concentrated, through bio-accumulation (Bank, 2012; Liu et al., 2012; Al Mukaimi, et al. 2018a). The anoxic conditions found within estuarine habitat conditions enhances the creation of methylmercury, which, out of Hg's other forms, is the most bio-accumulative toxin (Bank, 2012; Clampet, 2012; Eagles-Smith & Ackerman, 2014).

Exposure to high concentrations of organic Hg can affect animals by causing a reduced reproduction rate, slower growth and development, and, or, death (Yanko et al., 1994, 1998, 1999; Brunner et al., 2013). Consumption of contaminated fisheries or animals can cause harmful exposure to humans (Morse et al., 1993; Liu et al., 2012; Day et al., 2013) . Such health effects can include: damage to the brain, heart, kidneys, lungs, immune system, and the development of unborn babies in the womb, or affect to their cognitive functions (EPA, 1997).

Hg and other contaminants have been introduced into the SJR Estuary through point and non-point sources, such as discharge from the Oxyvinyls® chloroalkali plant, as well as from atmospheric fall out and are the major historic

sources of Hg (Al Mukaimi, et al. 2018a). The Oxyvinyls® chloralkali plant along Patrick Bayou is a US EPA Superfund site and listed on the NPL, seen in **Figure 2.** The plants started operations in 1948 (Lester and Gonzalez, 2015) and is located along the lower most Buffalo Bayou, 5.31km west of the confluence of Buffalo Bayou and the San Jacinto Estuary, and 9.88 km up stream and west of Scotts Bay. Within the SJR, upstream of both Scott Bay and the confluence of Buffalo Bayou and the SJR (**Figure 2**) are, the San Jacinto waste pits (56,656 m^2) used for the disposal of pulp and paper mill wastes, built in the 1960s (EPA, 2015; Al Mukaimi, et al. 2018a). In the 1960s, the EPA listed the HSC as one of the top 10 most polluted areas in the United States (EPA, 1980). The highest recorded values (2374ng g-1) of contaminants input was identified close to the industrial point sources, such as the superfund sites; and decreases exponentially with distance away from the point sources (Al Mukaimi, et al. 2018a). Analyses of the sediment record reveals that chemical contamination in the SJR Estuary sediment became identifiable as early as 1900, peaking between 1940 and the 1980s, and then shows a decline thereafter (Al Mukaimi, et al. 2018a). During the peak in contaminants between 1960 and 1970s, the HSC experienced massive marine life kills causing the EPA to list HSC as a highly polluted waterway and triggering the use of EPA environmental regulations to force producers to reduce their point source discharges (EPA, 1980; Lester and Gonzalez, 2015; Al Mukaimi, et al. 2018a). Sediment quality since 1970 has shown an improvement, with the

exception of Hg, which could be the result of non-point source inputs such as sewage and urbanization (Balogh et al., 1999; Al Mukaimi, et al. 2018a).

Estuaries like the SJR estuary and HSC system act as efficient filters and sediment traps, trapping contaminants and preventing their transport to the open ocean (e.g. Dellapenna et al., 2003). Al Mukaimi et al., (2018A&B) was the first study to report the results from vibra cores collected in Scott Bay and found highly elevated concentrations of Hg (max 2500ng/kg), well above background concentrations (50ng/kg) (USGS, 1970) at a depth far deeper (90-120cm) than has previously been sampled (50-80cm) and identified in the vicinity (Morse et al., 1993; Wen et al, 1999; Santschi et al, 2001; Al Mukaimi, et al. 2018a). Even though Scott Bay is very sheltered and the cores had very limited evidence of bioturbation or other sediment mixing (Al Mukaimi et al., 2018A&B), other parts of Galveston Bay clearly are exposed and have experienced both bioturbation and physical mixing (e.g. Dellapenna et al., 2006). Bioturbation, as well as sediment resuspension from wave and ship wakes; sediment erosion from storm surges and flood water currents; and sediment disturbances from dredging and other anthropogenic activities, can all lead to the re-introduction of Hg into the water column. Once re-introduced to the water column, the sediment, along with the associated contaminants, can be transported long distances and may also go through multiple cycles of erosion and re-deposition. The net results are recurring availability of Hg for biological uptake and a greater chance of Hg cascading up to

higher trophic concentrations and ultimately, a greater risk of exposure to humans (Dellapenna et al., 1998; Wen et al., 1999; Al Mukaimi, et al. 2018a).

^{210}Pb Geochronology

The natural lead radionuclide ^{210}Pb ($t_{1/2}$=22.3 yr, Eγ=46 KeV) can be used to determine the geochronology of sedimentary processes and records of a variety of marine environments such as estuaries (Nittrouer et al., 1979; Santschi et al., 1999; Sharma et al., 1987; Dellapenna et al., 1998; Dellapenna et al., 2003; Yeager et al., 2004; M. Almukaimi, 2016). ^{210}Pb is derived from the decay of ^{238}U (Uranium). In the U-288 decay series, ^{210}Pb decays from Rn when released into the atmosphere, then removed from the atmosphere via precipitation that can be deposited into any aquatic or marine environment. With a half-life of 22.3 years, ^{210}Pb geochronology is a useful tool for the investigation of sedimentation rates over the past 50-100 years (Nittrouer et al., 1979; Santschi et al., 1999; M. Almukaimi, 2018a).

Benthic Foraminifera Ecology

Benthic foraminifera have an important global role in the biogeochemical cycles of organic and inorganic compounds (Hayes, 1981; Lee and Anderson, 1991; Yanko et al., 1991; F. Frontalini, R. Coccioni, 2008). These unicellular organisms are one of the most diverse and widely distributed of marine organisms (Sen Gupta, 1999; Murray, 2006; Noortje Dijkstra et al., 2017). They are easily fossilized in the sedimentary record (Alve et al., 2009; Dolven et al., 2013; Noortje

Dijkstra et al., 2017) due to their calcium carbonate shells (tests) that can be found preserved in a wide range of marine environments.

Foraminifera's short life cycle, abundance, and global paleoenvironmental association give them a high value as bio-indicators for monitoring stressful conditions resulting from both natural occurrences or anthropogenic accidents (Kramer and Botterweg, 1991; Alve, 1991, 1995; Yanko et al., 1994, 1998, 1999; Coccioni, 2000; Samir, 2000; Samir and El-Din, 2001; Debenay et al., 2001, 2005; Murray and Alve, 2002; E. Geslin et al., 2002; Armoynot du Chatelet et al., 2004; Coccioni and Marsili, 2005; J. Morvan et al., 2006; F. Frontalini, R. Coccioni, 2008; Alve et al., 2010; Brunner et al., 2013; Noortje Dijkstra et al., 2017).

Since Resig (1960) and Watkins (1961) initiated the use of benthic foraminifera as environmental pollution indicators, there has been a significant number of studies conducted into the use of benthic foraminifera to identify physical, chemical, and anthropogenic stressors. Particular stressors, for example, sea concentration change, abundance of heavy metals or other trace elements, may have a significant impact on estuarine environments when occurring at a higher concentration than is biologically essential (F. Frontalini, R. Coccioni, 2008). This may potentially be toxic to the foraminifera, inhibit their metabolism and protein synthesis resulting in local extinctions, assemblage modifications in abundance and diversity, "dwarfism" (F. Frontalini, R. Coccioni, 2008) and the development of test abnormalities (Alve, 1991, 1995; Kennish,

1992; Yanko et al., 1994; Geslin et al., 1998; Yanko et al., 1998). A controlled study conducted by V. La Cadre and J. Debenay (2006), over the course of one year, aimed to identify how heavy metal concentrations affected the foraminifera population recovery rates and chamber deformities. They concluded that under stressful conditions foraminifera take between 15-30 days to asexually reproduce but delay their initial chamber construction from previously being 20 days to now 37 days and take an additional 5-7 months for full growth.

Through these extensive studies a number of foraminifera species have been identified to have a strong correlation between an environmental stressor and response. For example, the ***Elphidium excavatum*** species flourish in an environment of high physical and chemical stressors such as turbidity (Polyak et al., 2002) and heavy metal contaminants (Sharifi et al., 1991; Alve and Olsgard, 1999; Dabbous and Scott, 2012;). These species are capable of adapting to harsh environments, and recolonizing rapidly when the toxicity conditions in an area improve (Corliss, 1985; Coroliss and Van Weering, 1993; Linke and Lutze, 1993; Wollenburg and Mackensen, 1998; Alve, 1999; Noortje Dijkstra et al., 2017). Other stress tolerant species include ***H. germanica*** that have been shown to co-exist with ***Elphidium*** species (Sharifi et al., 1991; Alve and Olsgard, 1999; Yanko et al., 1998; Alve et al., 2009), ***Lobatula lobatula*** that are tolerant to high turbidity and coarser grain size in relation to higher energy environments (Mackensen et al., 1985; Hald and Steinsund, 1998), and ***Bulimia marginata*** that

thrives in nutrient rich muddy sediments (Murray, 1991; Jorissen et al., 1992; Langezaal et al., 2005; Mojtahid et al., 2006).

Brunner et al. (2013) in a study on the effects of the Macondo oil spill on the estuarine environment of Mississippi and Louisiana, observed an elevated standing stock (hypertrophy) when toxicity was reduced. This enabled some foraminifera species, that were more toxin tolerant, to reproduce again. Benthic foraminifera test deformities, due to anthropogenic pollution types, have been reported through various studies (Yanko et al., 1998; R. Elshanawany et al., 2011; N. Jayaraju et al., 2011; and Brunner et al., 2013). The identification of benthic foraminifera in each of the cores gives an indication into the health and environmental shifts of the study area, either due to anthropogenic activities or large storms like that of Hurricane Harvey.

CHAPTER II: THE ENVIRONMENTAL AND POLLUTION GEOLOGIC RECORD OVER THE PAST CENTURY IN SCOTT, BAY

2.1: Introduction

In this chapter the research objectives are to determine how increased anthropogenic activity in the Scott Bay area, and if these shifts are evident in the benthic foraminifera record. The assessment of the environmental change has been determined through examination of Hg profiles, ^{210}Pb geochronology, changes in down core grain size distributions, loss of ignition (LOI) testing, and benthic foraminifera assemblage shifts. Through these analyses the following initial hypotheses were to be either supported or refuted:

H1: *Historic events, like that of the building of San Jacinto Dam or large hurricanes/storms, will be indicated by a decrease in sand or clay deposits, respectively*.

H2: *The increase in urbanization around Scott Bay will indicate an increase in mercury (Hg) concentration and therefore cause benthic foraminifera assemblages to show indication of stress.*

H3: *The installation of the dam caused a reduction in both freshwater and sediment input. As a result, Scott Bay became deeper, and the saltwedge migrated upstream. This is reflected in the sediment record as a shift from freshwater to brackish benthic foraminifera species.*

2.2: Methods

This study utilized various methods to analyze: ^{210}Pb geochronology, heavy metal (Hg) contaminant concentration trends, grain size distribution, LOI testing, and benthic foraminifera assemblage variations. Geochemical methods followed a similar protocol to that described by Nittrouer et al. (1979), Santschi et al. (1999) and Al Mukaimi et al. (2016). The micropaleontology method used was similar to that used by Brunner et al. (2013).

2.2.1: *Sub-Bottom Profiler; CHIRP Data Acquisition:*

Four Sub-bottom profiler lines were acquired in 2016 across Scott Bay using an Edgetech 216 CHIRP system using a swept frequency range of 2-16 kHz. The CHIRP data was used to select optimal locations for sediment coring, by finding the thickest deposits of bay fill. Lines were positioned using a hand-held GPS with a navigation data stream fed into the CHIRP acquisition computer. The data were interpreted using the SonarWiz® software, where select horizons were digitally mapped.

2.2.2: *Core Collection and Processing:*

Two vibra cores were collected from Scott Bay on August 2, 2016 using a PVL Tech submersible vibra-coring system. Core locations SB1 and SB2 in Scott Bay, were chosen to be directly over the track of a CHIRP line where CHIRP data revealed continuously layered and undisturbed laminated strata, indicating no stratigraphic disturbance. The two cores penetrated to a depth of approximately 3.5m below sea bed. Recovered core lengths were 298 cm (SB1) and 289 cm

(SB2). Aluminum core barrels with a diameter of 7.62 cm were extracted, sealed upon recovery and stored in a large freezer at a temperature of 4°C to await processing. In the laboratory, each core section was split lengthwise where one half was to be sampled and the other half preserved intact for archive storage. For processing, core SB1 was cut into 3 sections and core sample SB2 was cut into 2 sections for ease in handling. Digital photographs were taken of each section, with over lapping photographic intervals, and a visual core log description of the lithology was created using Adobe Illustrator. The two 2016 pre-Hurricane Harvey cores were sampled every 5cm with additional samples collected from features of interest identified in the core for: geochronology, or heavy metal and hydrocarbon contaminant concentrations.

2.2.3: *Water and Organic Content Analysis:*

All samples were placed in pre-weighed aluminum tins. The samples and tins were weighed and then placed in an oven at 50°C for 24 hours, and were then re-weighed to measure sediment water content.

The same samples were then prepared for LOI and placed in another oven for 4.5 hours at 550°C to burn off organic content. After the samples had cooled, they were re-weighed to determine organic content. All sample measurements were recorded in an Excel spread sheet. The loss ignition method typically contains an error of maximum ±2% at 550°C (Heiri, O., et al., 2001; van Hengstum, P. J., et al., 2011).

2.2.4: *Grainsize Analysis:*

Grain size analyses of 2016 sediment samples were produced using the Malvern Mastersizer 2000 following the methods of Almukaimi et al., (2016). Following these methods, the 2016 pre-Harvey cores 5 cm intervals and target layers samples were analyzed for grain size distribution using the Malvern Mastersizer 2000. The system measures the light scatter density in a liquid medium from a laser to determine the particle size distribution of the sediment particles. Before adding the sample to the system, 2-4 g of wet sediment were homogenized and placed in a test tube and then 10 mL of a dispersant solution (sodium hexametaphosphate) was added. This solution was mixed using a vortex mixer machine to thoroughly separate the sediment particles in water. Since the Malvern can only accept particles no larger than 2000 μm, the samples were poured through a 2 mm sieve and then placed into the system until the allowable concentration of sediment, or obscuration concentration, was achieved. The system provided output measurements of the average sand, silt, and clay fractions of each sample that was exported to Excel (Al Mukaimi et al., 2018).

2.2.5: *Total Mercury (Hg) Analysis:*

In order to use a Direct Mercury Analyzer (DMA-80) for the analysis of the total Hg concentration present, samples were dried, and ground into a powder of homogenized sediment. All sample concentrations were put through the test procedure. This required the use of several sample standard tests to be run in addition to the actual sediment samples. This ensured the reliability and

consistency of the results due to any loss of Hg as a result of the chemical reactions between the acids in the machine and the nickel boats in which the samples were placed. The standard for this test is the Certified Reference Material (CRM) a MESS-3 (0.091 ± 0.009 ppm Hg) marine sediment standard from the National Research Council of Canada. The standards typically had a difference of at most ± 0.006 mg/kg. Among the actual sediment samples and standard samples, a few of the system's sampling boats are left empty as blanks so to make sure there is no cross sample contamination, as well as to ensure accuracy as the samples go through analysis. Every tenth samples for each system run was duplicated to verify results. A total of 30 sediment samples, 3 blanks, and 6 MESS samples made up each system run (Almukaimi, 2016).

The Direct Mercury Analyzer (DMA-80, milestone srl, Italy) is operated in compliance with the US EPA Method 7473 for the analysis of mercury in solids through thermal decomposition, amalgamation, and atomic absorption spectrophotometry (EPA, 1998). The machine first thermally decomposes the samples in a controlled furnace so as to release the mercury from the sediment. The flow of oxygen through the furnace carries away the decomposition products to a hot catalyst at 615 °C. This reduces the trapped halogens, nitrogen, sulfur oxides and all mercury species to its elemental form. The Hg, in its vapor form, is carried with oxygen to a gold amalgamator for it to be selectively collected. The amalgamator is then heated to 900°C leading to the release of the Hg vapor to be carried away to hot curet cells (125°C) for atomic absorption spectrometry. The

Hg is quantified by its absorption at 253.7nm wavelengths which is a function of Hg concentration (Almukaimi, 2016). The standard MESS-3 needs to be within a certified range and average recovery rate of 97 % ± 7 % (Mean ± RSD, n = 137). Results were then exported to Excel.

2.2.6: *^{210}Pb Radioisotope Geochronology:*

For Total and Excess ^{210}Pb geochronology analysis, the same 5cm interval samples were wet sieved through a 63μm sieve, dried, and ground into a powder of homogenized sediment. The larger surface area of the size fraction of clay and silt allows for higher absorption and, therefore, concentration of the radioisotope (Nittrouer et al, 1979). Following the methods of Nittrouer et al (1979), Santschi et al., (1999), and M. Almukaimi et al., (2018) the activity of ^{210}Pb (t 1/2 = 22.3 yr, Eγ= 46 KeV) was measured using the granddaughter ^{209}Po from the same decay series. Approximately 1g of the dried sample was added to a beaker and spiked with 0.25μl of the known activity of ^{209}Po tracer. Using 15ml of concentrated HCl and HNO_3 was added to the beaker for the digestion of the samples. The acid samples were then placed on hot blocks to be evaporated to near dryness. When close to dry, 15ml of concentrated HCl and HNO_3 was added and the procedure repeated. 15ml of HCl was then added, and samples baked until practically dry, at that point 50ml of 1.5 M HCl and ascorbic acid was added to the samples and stirred with a glass rod after being taken off the hotblock. A silver planchet was then prepared, with a small piece of tape placed on one side only, and put it into

the container with the acid and the now digested sample. The used container included a magnetic stir bar to be stirred for 24 hours at which point the radioisotope becomes electroplated onto the silver planchet. On completion, the silver planchet was removed and cleaned with acetone and deionized water prior to counting by alpha spectroscopy using a Canberra DSA-1000 16K multichannel surface barrier detector. The measured ratio between the Po isotopes and the relative activity of the radioisotope spiked sample determines the ^{210}Pb activity. The excess lead is calculated by the difference between the total and supported activities which is determined from the constant ^{210}Pb activities at depth (M. Almukaimi, 2016). By calculating the sediment accumulation rate, the geochronology of the samples can then be determined.

In order to achieve these results, some assumptions about ^{210}Pb needs to be made, such as the addition of ^{210}Pb that has remained constant at the sediment water-interface. This is a static chemical, and the reworking rate of the radioisotope is nonexistent (Sharma et al, 1987 Santschi et al, 2001; M. Almukaimi, 2016). With the sediment accumulation rate and specific activity of ^{210}Pb being constant when buried, the decay is assumed to be exponential and the following calculation can be used:

(Eq.1) $$Pb^{210}xs(z) = (Pb^{210}xs(0))exp(-\alpha z)$$

$$S = \lambda\alpha$$

Where ($^{210}Pb_{xs}$ (z)) and ($^{210}Pb_{xs}$ (0)) represent the excess ^{210}Pb concentration at the corrected depth (z) and at the sediment interface, (S) = the linear

sedimentation rate (cm y^{-1}); (λ) = the decay constant of ^{210}Pb (0.031 year -1) and Alpha (α) = the slope defined by a regression through the data (Dellapenna et al, 1998; Santschi et al, 1999; Santschi et al, 2001; M. Almukaimi, 2016).

2.2.7: *Approximate age date Calculations:*

The approximate age calculations were calculated using Equation 1 to then determine the accumulation rate over time. Using the overall accumulation rate per year from the decay of the surface activity to core depth of background activity concentrations, time versus depth was then calculated to give the approximate year date. This “steady state accumulation rate” is created under the assumption that the decay of ^{210}Pb remains constant and no reworking of the sediment interface has occurred.

2.2.8: *Gas Chromatography-Mass Spectrometry (GC/MS) Analysis:*

Six target layers were identified as possibility containing hydrocarbons in the 2016 pre-Hurricane Harvey cores and sub-sampled or Gas Chromatography-Mass Spectrometry (GC/MS) analysis. The samples were placed in a vial and sent to the Geochemical and Environmental Research Group (GERG) at College Station for GC/MS testing, looking specifically for Polycyclic aromatic hydrocarbon (PAHs) concentrations. The GC/MS method followed was as described by Knap et al. (2017). To keep the results within the calibration curve, an appropriate dosing technique was used, where the sample is partitioned from a solvent solution into a biocompatible polymer, in this case, polydimethylsiloxane (PDMS).

For successful dosing, an excess mass of hydrocarbon in both the loading solution and PDMS O-ring reservoirs, is needed to prevent depletion during the exposure duration affecting the target concentrations. The PDMS O-rings are loaded with 1-MN of Acros Organics (97%) in a Fisher Scientific HPLC grade methanol solvent. Care was taken to ensure the correct partition coefficient was used for the environmental testing conditions of each dosing vessel. The concentrations of 1-MN were calculated from Total Scanning Fluorescence (TSF) using a Aqualog Horiba Fluorometer and then verified by GC/MS.

After the dosing experiments, 1 L of liquid sample was extracted and surrogate standards were added. These extracts were spiked with internal standards. The samples were then measured by selection ion monitoring using a 30 m x 0.25mm i.d. (0.25 μm film thickness) fused silica capillary column, fitted into an Agilent Model GC/MS, with an oven temperature of 60°C to 300°C for 6 minutes (Knap et al., 2017).

2.2.9: *Micropaleontology Analysis:*

Due to length of run time for this analysis, it was decided to only use samples from core SB1. For each sample from core SB1, 1.25-2.5 cm^3 was taken and sieved to preserve grain sizes at >63 μm. The samples were then placed in clean glass beakers to be dried in an oven over night. The benthic foraminifera identified in each sample were then picked and sorted by species into standard 60-box micro paleontological slides. Taxonomy present were identified and counted using a scanning electron microscope. Where

deformed species are found those too will be counted and sorted to species as closely resembling as possible. Severely deformed individuals can be near impossible to identify to the species level.

Morphological attributes of foraminifera tests abnormalities that indicate "stressed" and will be counted as deformed are as follows (Brunner et al., 2013; Yanko etal., 1994):

1. Change in coiling direction,
2. Change in axis coiling,
3. Misshapen chambers/ protuberances,
4. Multiple apertures,
5. Chamber inflammation,
6. Conjoined twinning, and
7. Deterioration of tests

Benthic foraminifera deformations and taxa of each sediment layer were compared to the results from the Hg and Pb^{210} and other contaminant content analyses, in order to be considered against the study hypotheses.

2.2.10: *Geographical Information Systems (GIS):*

ArcGIS was used to analyze aerial photography from the Texas General Land Office (TGLO) to identify historical land form and use changes to illustrate the impact of anthropogenic activity.

For the post-Harvey 2017 study, several maps of the distribution of storm layer thickness, Hg concentrations, and benthic foraminifera assemblage

distribution, were created to understand how SJE sediments and benthic foraminifera communities were affected spatially by Hurricane Harvey's large flux of freshwater to the system.

2.3: Results

2.3.1: ^{210}Pb Geochronology

Cores SB1 and SB2 were collected approximately 800m apart, with SB2 being collected at the same core site of Al Mukaimi et al. (2018) core C-22. The SB1 and SB2 excess ^{210}Pb profiles (**Figure 3**) have very similar shapes, with two intervals of nearly uniform activity below which there is a sharp decrease in activity. Al Mukaimi et al. (2018)., reported an accumulation rates, based off of both ^{137}Cs and ^{210}Pb of 1.5 cm y^{-1}. The sediment accumulation rate, using the same approach as Al Mukaimi, for Core SB2 was also calculated to be 1.5 cm y^{-1}, based off of ^{210}Pb and core SB1, which was collected 800m to the northwest, also within Scotts Bay, has a ^{210}Pb accumulation rate calculated to be 1.7 cm y^{-1}. The ^{210}Pb profiles have intervals of relatively uniform activities down core indicating that the sediment was deposited in a sequence of episodic events and also that there was likely sediment reworking associated with each of these events. Consequently, although a decadal scale sedimentation rate can be determined, dates cannot be determined for specific layers or events based solely off of the ^{210}Pb geochronology. Due to the close comparison between Al Mukaimi et al. (2018) core C-22 sample and the SB1 and SB2 samples, the ^{137}Cs

maximum nuclear bomb fallout in 1963 found at a depth of 75 cm in C-22 can also be correlated across the other two cores.

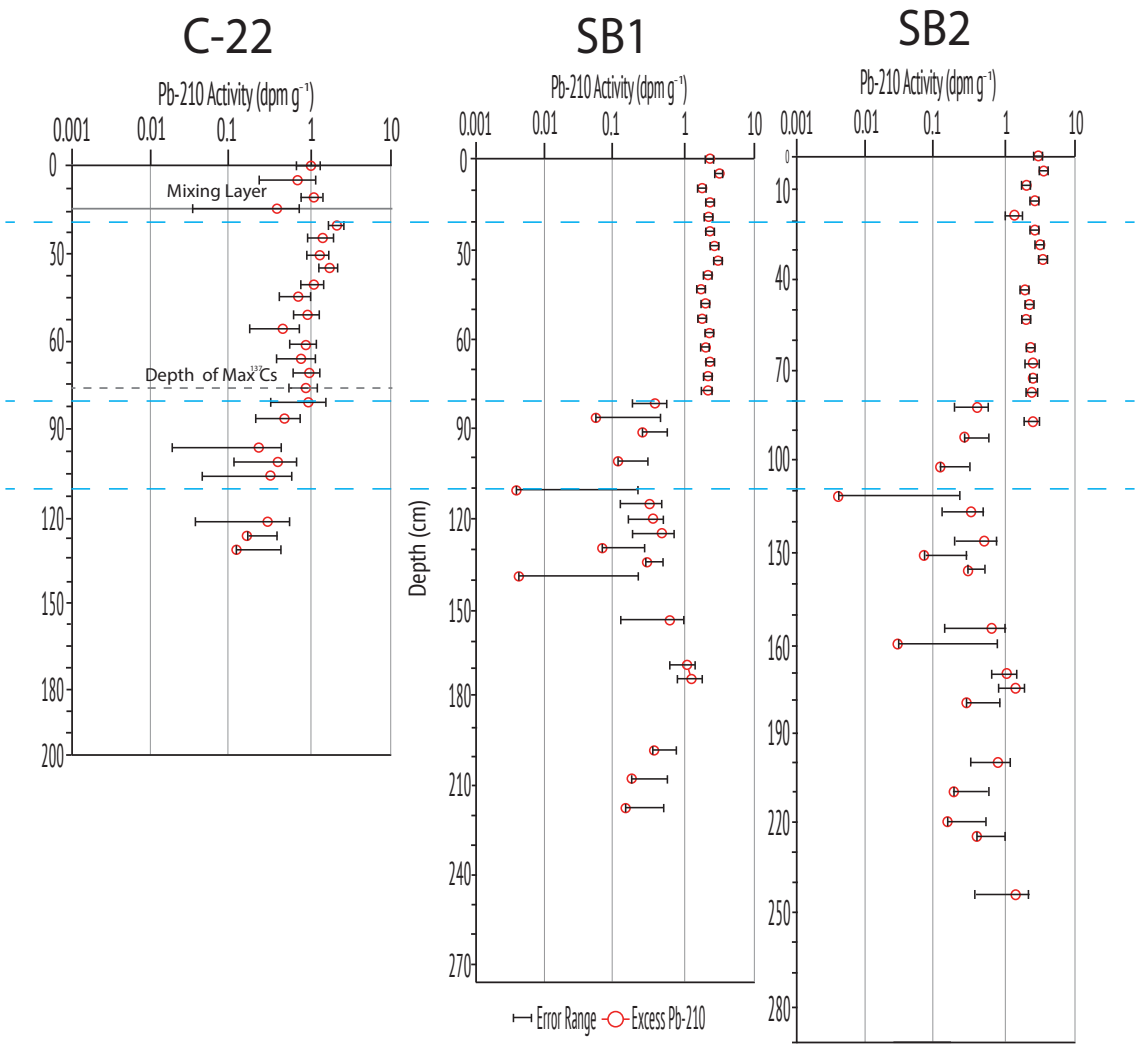

Figure 3: ^{210}Pb comparison between a core sample collected Scott Bay by Al Mukaimi et al. (2018) in 2014, and the two cores collected in 2016 for this study. Max 137 Cs, indicates the fallout maximum of Cesium during the atmospheric nuclear bomb testing testing.

2.3.2: *Grain Size*

2.3.2.1: *SB1 Core*

Grain size analyses of the core SB1 reveals 3 distinct lithological units (**Figure 4**). which are:

1) A basal sand dominated interval (140-275cm) consisting of greater than 75% sand, with the remainder consisting of silt dominated mud;

2) A mud dominated layer (80-140cm) dominated by silt and clay, with a minimum of ~2% sand at 120cm, and bookended with sudden increases in percent sand of about 90% at 140cm and ~60% sand at 80cm;

3) A sand dominated layer (50-80 cm) generally consisting of greater than 60% sand and silt dominated, with a maximum percent sand of ~80% at 55cm;

4) A surface layer (0-50 cm) consisting of a relatively even mixture of silt and clay with about 10-30% sand in the upper 35 cm, and ~40% sand within the 35-50 cm interval.

2.3.2.2: *SB2 Core*

Grain size analyses of Core SB2 (**Figure 5**) reveals two distinct lithological units, which are:

1) A basal sand dominated interval (170-289cm) generally consisting of greater than 45% sand, with the remainder consisting of silt dominated mud; and

2) A surface layer (0-170 cm) consisting of a relatively even mixture of silt and clay, generally less than 10% sand with slight mixing of up to 20% sand.

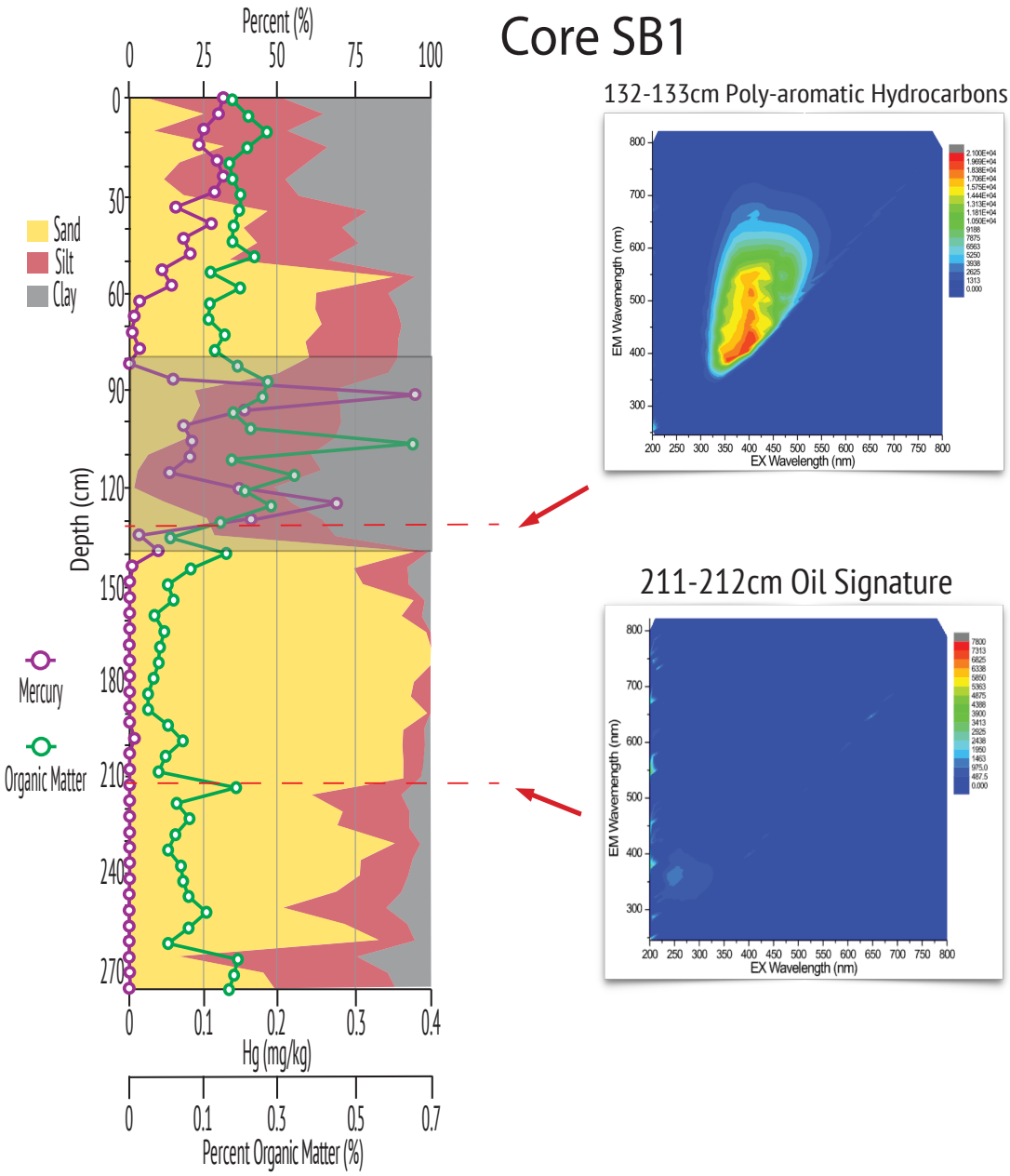

Figure 4: Pre- Harvey 2016 SB1 core results depicting; grain size distribution, organic matter, and mercury content. Two GC/MS results at 132-133cm and 211-212cm, provided by GERG at Texas A&M University, indicating hydrocarbon signatures. Clay dominated facies iodinated by shaded grey area.

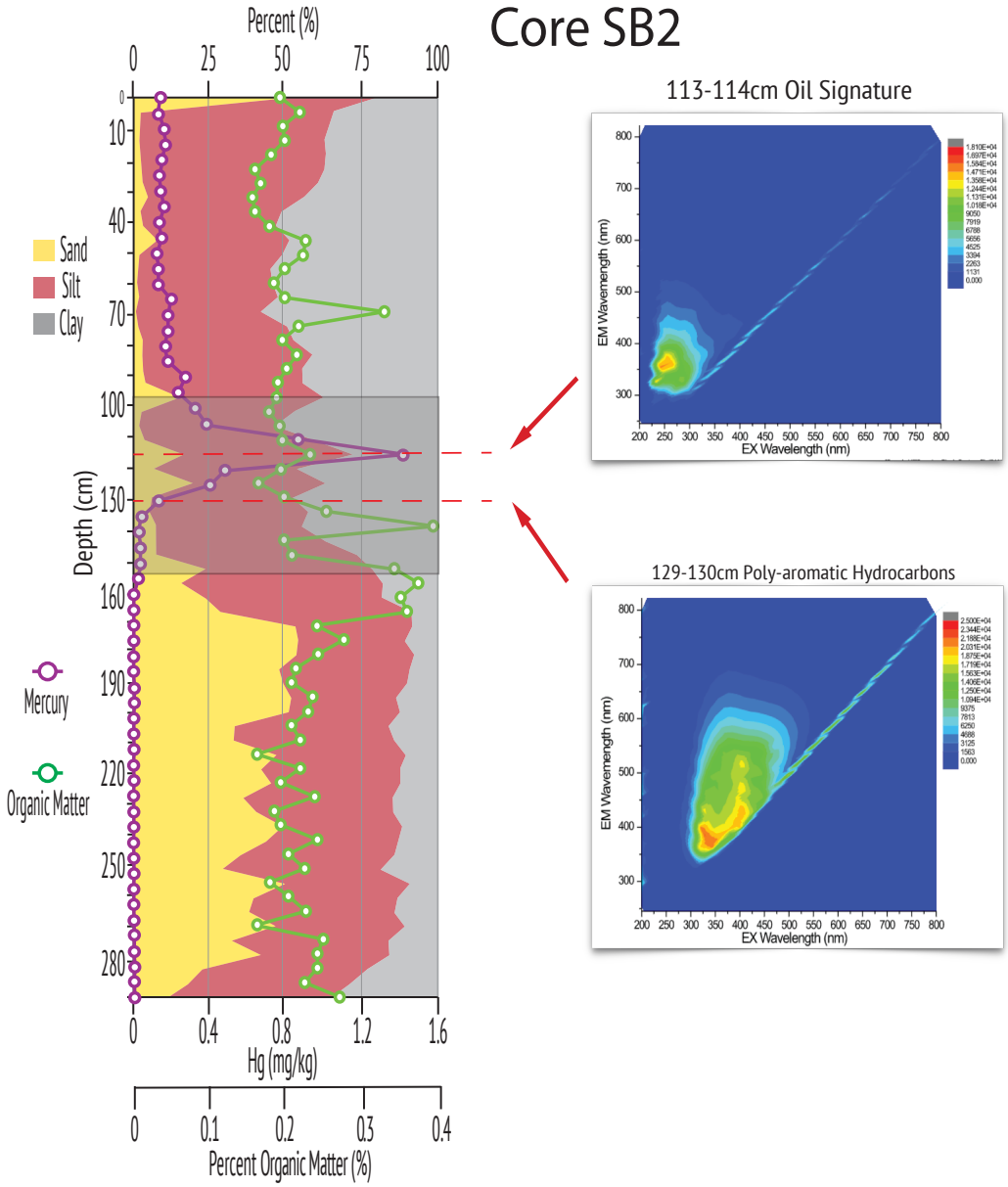

Figure 5: Pre- Harvey 2016 SB2 core results depicting; grain size distribution, organic matter, and mercury content. Two GC/MS results at 113-114cm and 129-130cm, provided by GERG at Texas A&M University, indicating hydrocarbon signatures. Clay dominated facies iodinated by shaded grey area.

2.3.3: *Geochemistry*

In core SB1, indicated in a shaded gray (80-140cm) (Figure 4), Hg concentrations are observed to fluctuate drastically. From the bottom of the core, upward, the Hg concentrations remain around 0.0038mg/kg until the first spike at 130 cm with a concentration of 0.275mg/kg. At this interval, a change in grain size is observed, changing from sand to clay dominated. Further up the core at 105cm a peak of organic matter is seen to have increased in concentration from 0.2% to 0.6%. Then at 95cm the Hg peaks with a maximum concentration of 0.378mg/kg, all within the clay layer, before the Hg and clay decrease.

Within this (80-140cm) gray zone of interest, a target layer that was identified and sampled for GC/MS at 132cm, resulted in a large spike in PAH concentration as high as 5132.93ng/g in Fluoranthenes/Pyrenes. This is 5000 times background water concentrations of 4ng/L (Mumtaz, M., & George, J., 1995). At 211cm, another target sample was analyzed for GC/MS. This indicated a slight Estimated Oil Equivalent (EOE) signature of 578.09μg/L.

In core SB2 (**Figure 5**), the gray area of interest (95-155cm) indicates only one large Hg peak at 115cm of 1.4157mg/kg, about three times greater than the highest concentration of Hg found in core SB1. Above the peak, at 100cm the Hg concentrations range from around 0.1-0.2mg/kg, whereas down core from the identified peak the Hg concentrations remained consistently below a minimum threshold of 0.004 mg/kg.

At 129-132cm two target samples were tested and a significant spike of PAHs was found, with concentrations as high as 6380.45ng/g (129cm) and 4503.7ng/g (132cm) in Fluoranthenes/Pyrenes. Further up core, at 113cm a target sample for GC/MS resulted in a substantial signature of EOEs, with a concentration of 28,299.54μg/L.

2.3.4: *Biostratigraphy*

Variations in the benthic foraminifera community structure, as seen in the profile from core SB1 (**Figure 7**) suggest three separate communities, which correlate well with the lithological units identified from the grain size data. Between

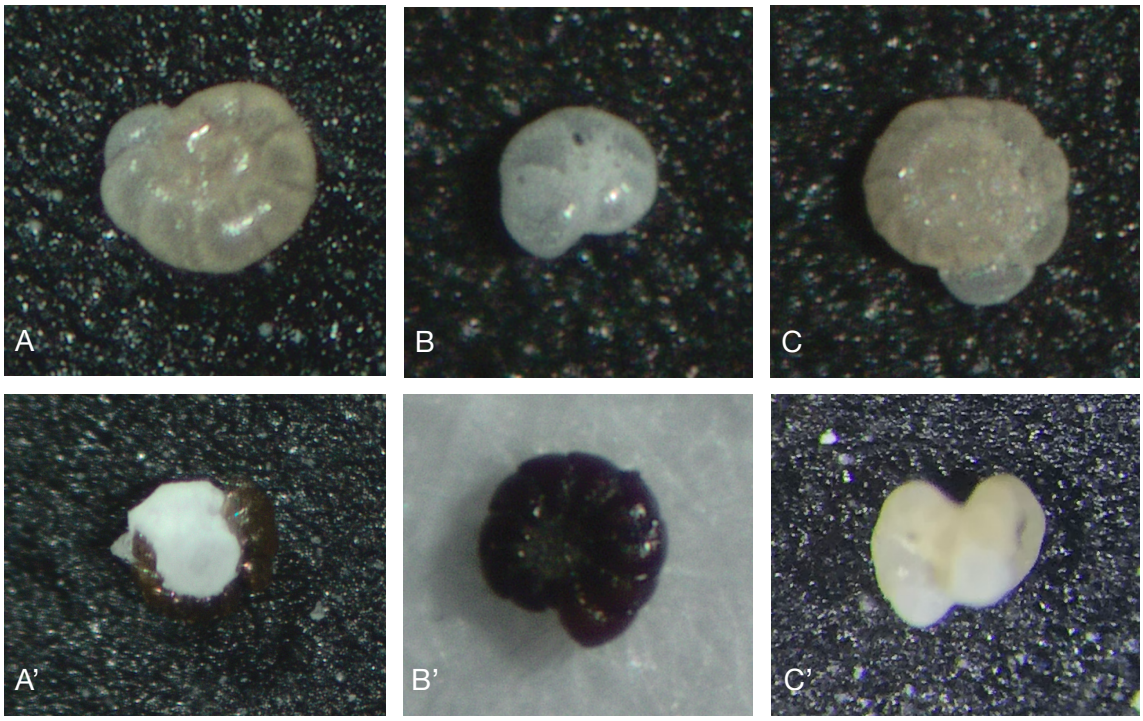

Figure 6: Examples of "stressed" benthic foraminifera. A; *Ammonia beccari* individual with test (shell) degraded down to membrane. B; *Elphidium poenyum* individual's test color changed from off-white/clear, to a dark brown. C; *Ammonia beccari* individual having grown a test deformity of a conjoined twin.

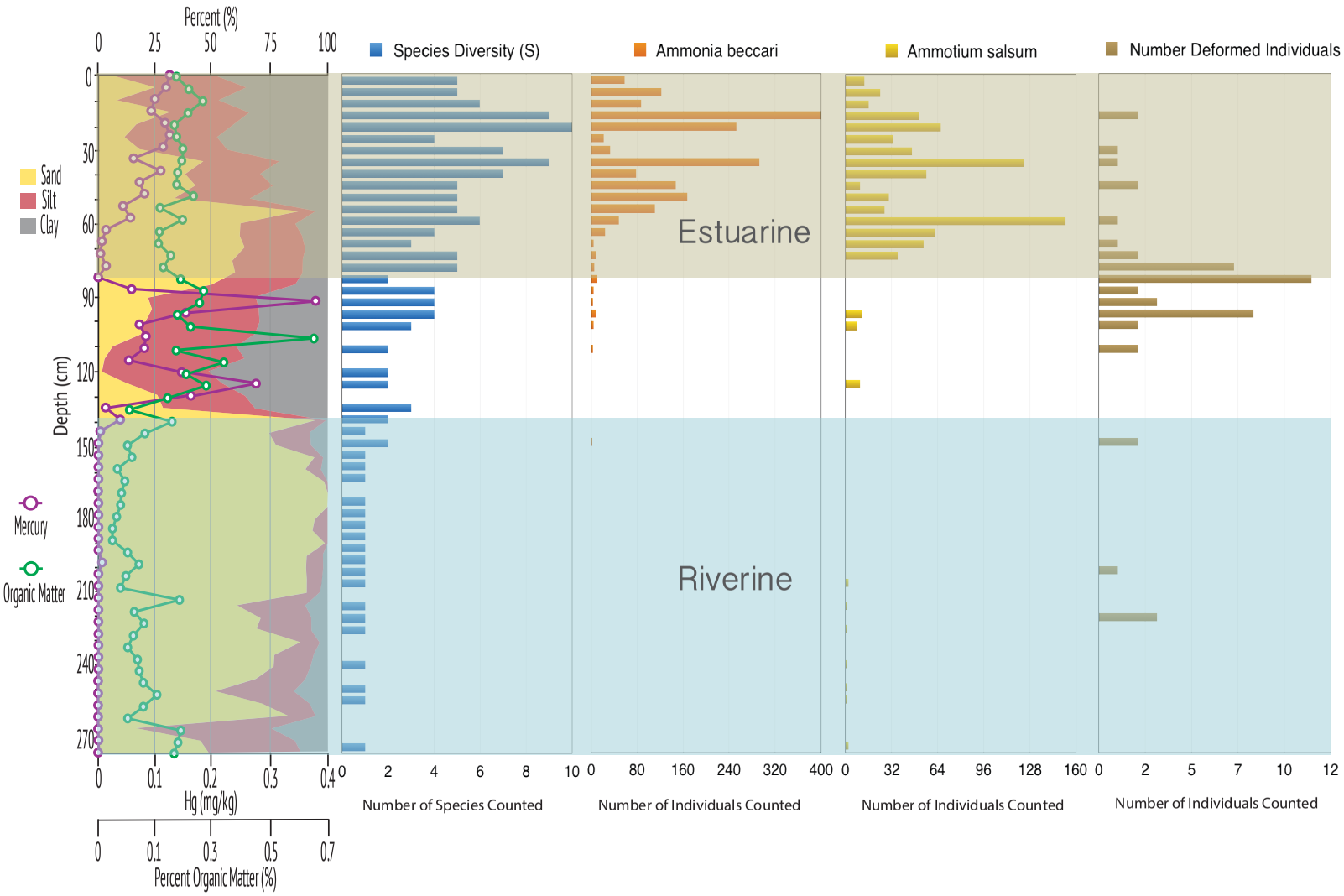

Figure 7: Pre- Harvey SB1 core results depicting; grain size distribution, mercury content, and micropaleontogical analysis, indicated through key benthic foraminifera individual species counts.

140- 275cm very few foraminifera species were found. At 219cm, c 1946±3, of the few foraminifera that were represented, 100% of those individuals indicated signs of “stress” (**Figure 6**). This was in close proximity to the EOE signature (211cm) also found in SB1. In the section between 70-100cm, the foraminifera record show the greatest fraction of stressed tests, with a peak at 80 cm, indicating about a 10cm lag in response to the peak Hg concentration at a depth of 90cm.

At a depth of 100cm, there is an increase in the benthic foraminifera species diversity, increasing steadily to the top of the core. Further up the core at a depth of 70cm a shift in ecology occurs, beginning with an increase in *Ammotium salsa* species, and then at 60cm *Ammonia beccari* begin to be prominent in the record. These two well represented species are common in brackish estuarine environments and remain as the dominant species up section, for the remainder of the core.

2.4: Discussion

2.4.1: *Anthropogenic Influences vs Historic Records*

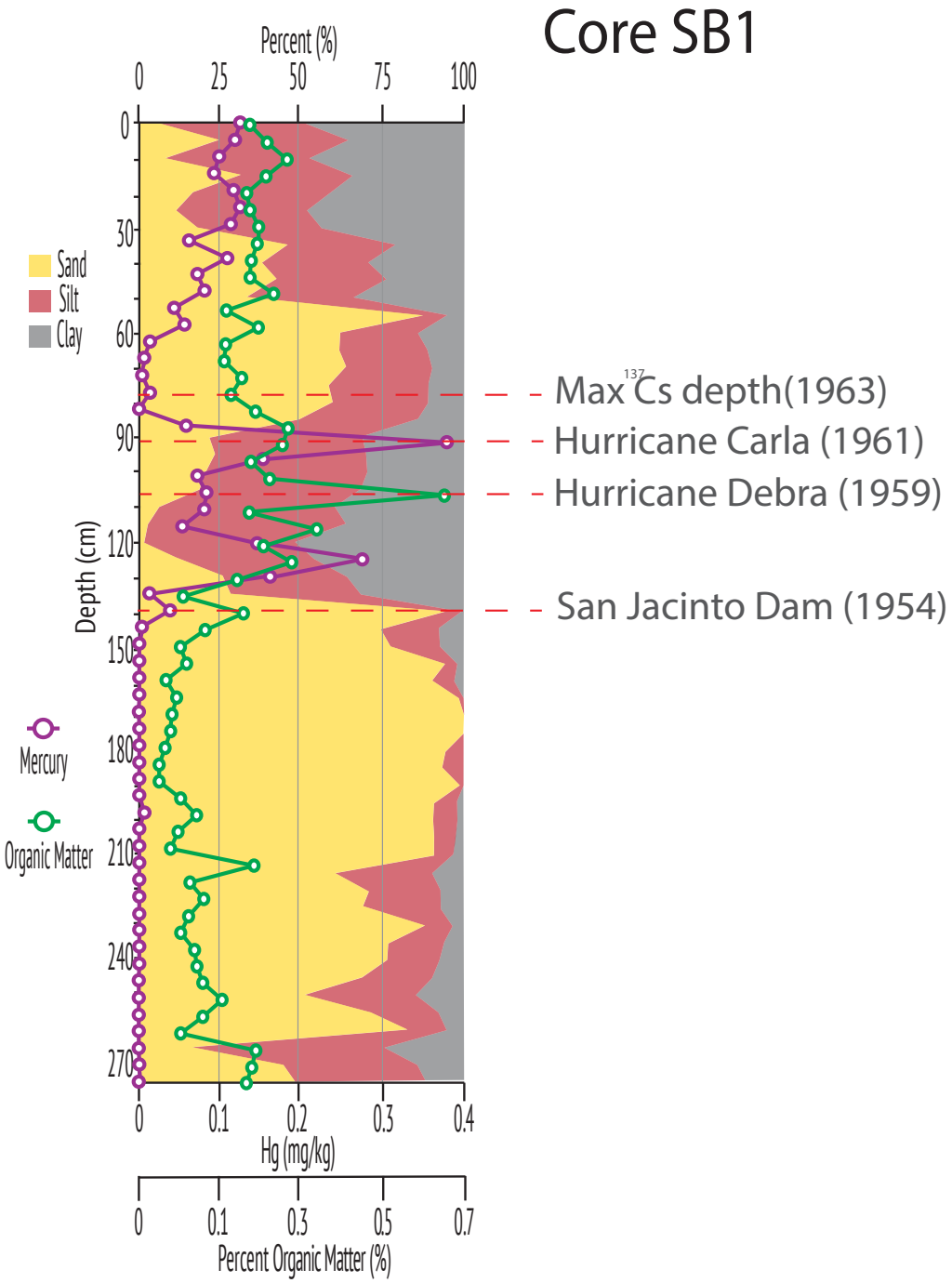

Figure 8: Pre- Harvey SB1 core results depicting; grain size distribution, organic matter, and mercury content in correlation with historic events, both anthropogenic and natural. Max ^{137}Cs, indicates the fallout maximum of Cesium during the atmospheric nuclear bomb testing testing.

Anthropogenic influences in Scott Bay area recorded in the sediment can be correlated to the historical records of significant impacts to the area (**Figure 8**). There have been multiple studies performed in the area on anthropogenically caused subsidence (White et al., 1993; Coplin and Galloway, 1999; Santschi et al., 2001; USGS, 2002; Byun et al. 2004; Ravens et al., 2009; Al Mukaimi et al., 2018a, and Al Mukaimi et al., 2018b). These studies conducted since 2012, have indicated that the Scott Bay area has experienced up to a maximum of 2.59cm/yr of sedimentation (Al Mukaimi et al., 2018a, and Al Mukaimi et al., 2018b). The HSC area has also experienced about 3m of subsidence since 1944 and greater than 3m since the 1920s.

Since the induction of the Clean Water Act in 1972, a Texas legislative group was created in 1975 called Harris-Galveston Coastal Subsidence District, to regulate groundwater withdrawal. Until then ground water was the primary source of water to the urban area, which then shifted to Lake Houston after the building of the San Jacinto Dam was completed in 1954. With the dam in place, a further decrease in sediment and freshwater supply transported downstream would be expected. As seen in **Figure 8** and **9** the grain size analysis shows a sudden change in grain size from sand to clay, this can be correlated to the building of the San Jacinto Dam in 1954.

While the area has been heavily affected by industrial and other human impacts, it is also prone to Hurricanes and tropical storms that hit the area frequently. Since the 1950s about 64 large strength storm systems have hit the

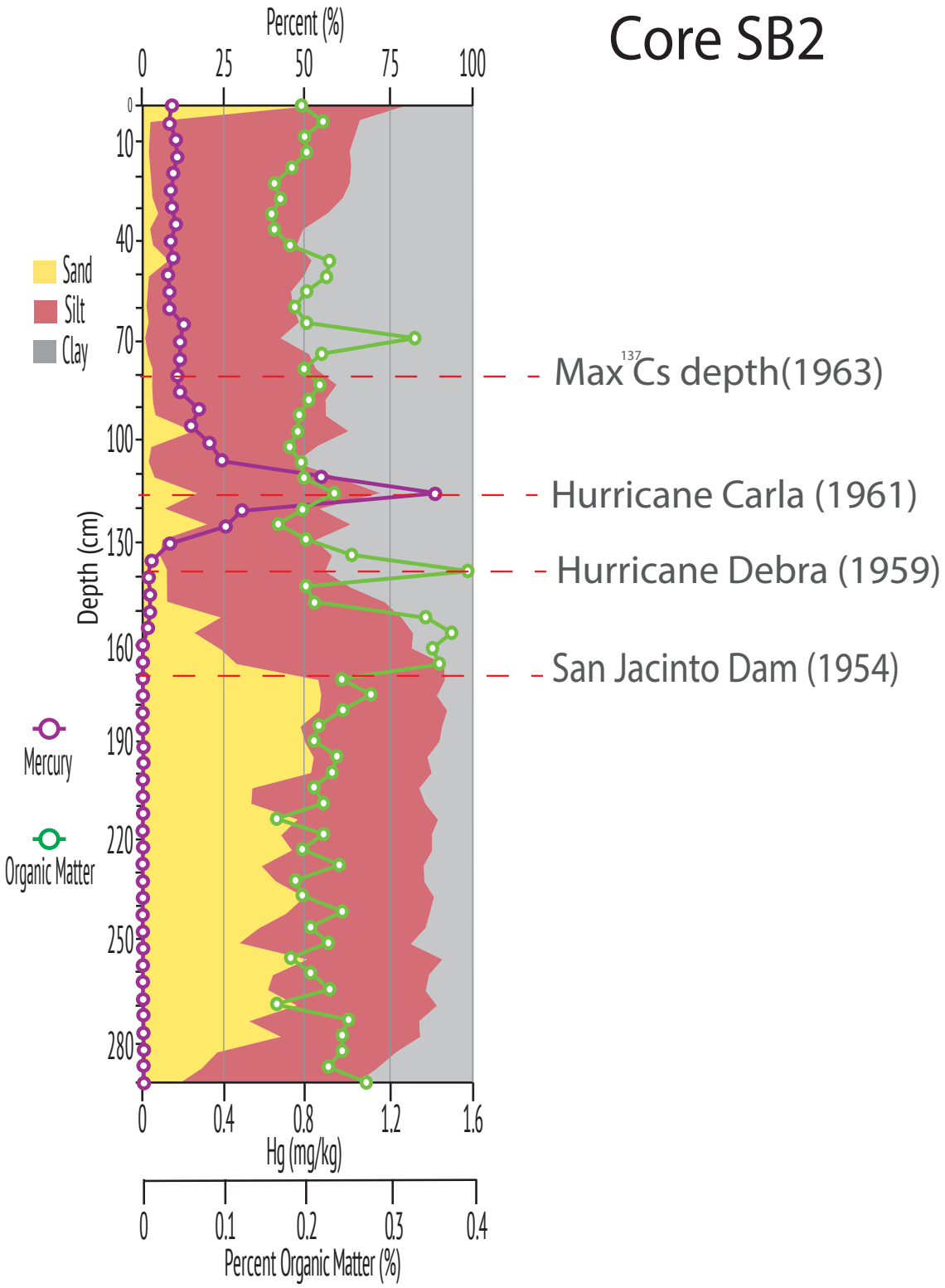

Figure 9: Pre- Harvey SB2 core results depicting; grain size distribution, organic matter, and mercury content in correlation with historic events, both anthropogenic and natural. Max ^{137}Cs, indicates the fallout maximum of Cesium during the atmospheric nuclear bomb testing testing.

Texas coast (Roth, D., 2010). The majority of large storm systems hitting the area result in 3m storm surges of up to 4.5m inundating coastal cities and local ecosystems. However there were only two large storms reaching landfall between the building of the San Jacinto dam in 1954 and the max Cs nuclear bomb fall out occurring around 1963, with a significant enough rainfall in the San Jacinto Estuary area to cause a man flux of freshwater downriver to affect the core locations.

In 1959 Hurricane Debra made landfall with wind speeds up to 136 km/h and 9.19 cm of rain a day causing the Galveston causeway to be completely flooded resulting in the Galveston Island being temporarily detached from the mainland. Such a flux of freshwater could cause erosion of contaminant bearing sediment from upstream SJE to be transported and deposited in the semi-sheltered Scott Bay. This can be correlated to the organic matter peaks found in both cores seen around 105cm (SB1) and 135cm (SB2).

A few years later Hurricane Carla hit the greater Houston area in 1961 with 270 km/h winds accompanied by a 3m storm surge and 17.41cm of total rainfall. This can be correlated to the same depth as a significant spike in Hg concentration in both SB1 (90cm) and SB2 (115cm), which also correlates to the biostratigraphy in **Figure 11**, where a strong presence in “stressed” foraminifera individuals, indicates a significant event. This is consistent with a flux of pollutants or rapid salinity and temperature changes.

Figure 10: Hurricane Alicia (1983) destruction of Scott Bay, Brownwood neighborhood (White et al., 2003). Picture from Harris-Galveston Coastal Subsidence District

The neighborhood of Brownwood, on the north side of Scott Bay, became completely inundated with a 3.3m storm surge from Alicia (White et al., 2003, **Figure 10**). The loss of Hg concentration in the sediment at around the same age in both cores could have been caused by erosion, suggesting that the Brownwood neighborhood and subsequently Scott Bay, may have also been flooded with previously buried contaminants, as well as causing land pollution and debris to enter the water system to cause such a stressful environment for the benthic foraminifera communities. Due to the ongoing subsidence and relative sea concentration rise in the region, once the storm surge receded, the neighborhood remained underwater causing the area's homes to be abandoned. The area has now been returned to a wetland restoration reserve called Brownwood Park.

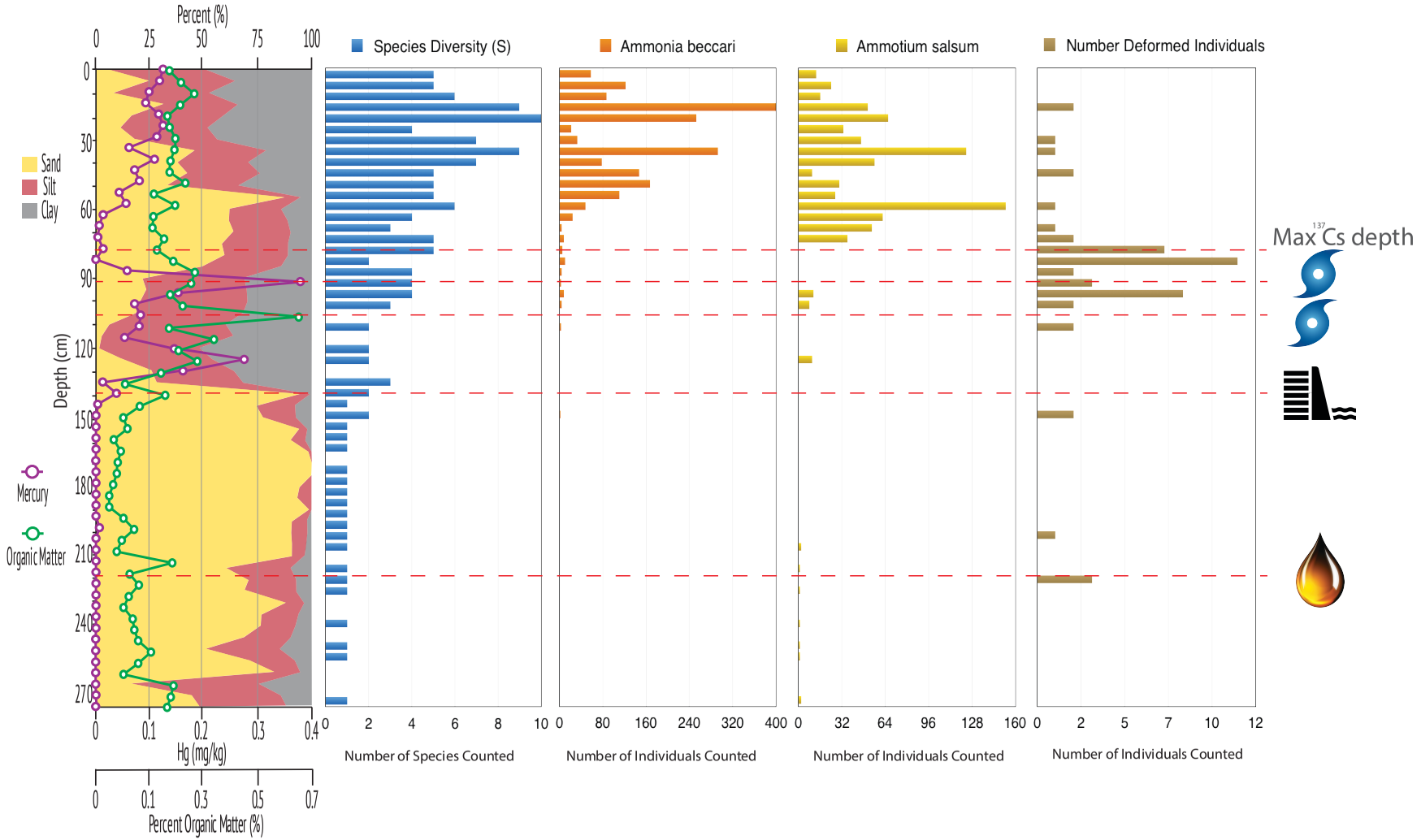

Figure 11: Pre- Harvey SB1 core results depicting; grain size distribution, mercury content, and micropaleontogical analysis, indicated through benthic foraminifera individual counts with a comparison to historic storm records and other chemical indicators.

According to the IPCC, observed global eustatic sea level rise is about 0.26-0.55cm/yr, where as the relative sea concentration rise of the HSC area has been about 2.78cm/yr due to the combined effects of eustatic sea level rise and ground subsidence (Al Mukaimi et al., 2018a, and Al Mukaimi et al., 2018b). For estuaries to persist, regardless of the rising sea level, there must be a balance between sediment accumulation and removal.

Looking at the sediment record provided in this study, there is clear evidence of change that can be correlated to the building of the San Jacinto Dam, and a linkage to storm event signatures in the record. Therefore, H1 hypothesis is supported with the statement that the building of San Jacinto Dam or large hurricanes/storms, can be indicated by a decrease in sand or clay deposits, respectively.

2.4.2: *Environmental Shift*

The evidence provided by the Benthic Foraminifera record indicate the affects that anthropogenic and environmental influences have had on the SJE (**Figure 7 & 11**). At a depth of 211cm, a strong presence of “stressed” foraminifera appear to correlate to a small hydrocarbon signature found through GC/MS at same depth in SB2. Another observation of high “stressed” individuals was also found from 75-105cm (SB1) which correlated to the sudden peak in Hg concentration (90cm, SB1). A similar delayed reaction was seen in a study conducted by V. La Cadre and J. Debenay (2006), where their controlled introduction of heavy metal concentrations to a benthic foraminifera community

revealed that high heavy metal concentrations create a delay in the foraminifera's construction of the first test chamber, from 20 to 37 days. Specifically they found the *Ammonia beccari* species first chamber became deformed after only 10 μm 1-1 of heavy metals was introduced, but once at a concentration of 200 μm 1-1 it had taken the foraminifera over 270 days to reproduce if they did at all. In this study, the reaction of the benthic foraminifera with a reduced species abundance at each heavy contaminated depth in the core, suggests that anthropogenic pollution can have immediate effects on the environment, creating an unhealthier system. This supports the H2 hypothesis: that benthic foraminifera respond directly to local pollution events by a reduction in species abundance.

In addition to foraminifera reacting to pollution events, when looking at **Figure 7 & 11**, at the same depth of grain size shift, there indicates to be an increase in species diversity. Having correlated the change in sediment input has been correlated to the building of the San Jacinto Dam. Due to the dam reducing the output of freshwater and sediment supply downstream, the subsidence seen in the HSC would have contributed to an increase in salinity. Therefore, seeing an increase in foraminifera species diversity and saline preferred species (*Ammonia beccari*, and *Ammotium salsum*) would also be anticipated with the building of a dam upstream.

Not only are the benthic foraminifera seen to be reacting to the anthropogenic impacts but also to large storm events. Around the Hurricane

Debra (1959), it appears that prominent benthic foraminifera species (*Ammonia beccari)* in the area increased in population after this event. Also, around this time, according to historical records, Galveston Bay experienced a number of large storm events. The increase in the brackish tolerant species is most likely due to the San Jacinto Dam preventing a large inventory of freshwater and sediment, the hurricane storm surge bringing in more saline tolerant species, and with the subsidence allowing the seawater to travel further upstream diluting the pollution, and providing more nutrients and preferable environment for those species (*Ammonia beccari*, and *Ammotium salsum*) to thrive in.

The two brackish species dominate the record above the storm layers, indicating that Scott Bay permanently shifted from a freshwater to a brackish/ estuarine environment. This is likely due the combination of the loss of freshwater inflow from the installation of the dam as well as enhanced subsidence/reduction in sediment input causing the Scott Bay to become deeper, allowing an upstream migration of the saltwedge. It is unlikely that these shifts in environmental conditions had any significant relationship to the storm, more likely that the timing is coincidental. This would provide evidence to support H3 hypothesis: that the benthic foraminifera shifted from freshwater to brackish dominated species. The further inundation of sea water into the area, with ongoing subsidence, San Jacinto Dam as a hinderance for sediment input, and landward salinity intrusion, will likely only move the tidal prism further upstream, causing greater wetland loss than has already been observed at the current time.

2.5: Conclusion

The large petrochemical industrial complex in close proximity to the HSC and the adjacent neighborhoods, has caused substantial anthropogenic impacts to the lower SJE and Scott Bay area. Over the past century the area has experienced an increase in urban expansion, resulting in a demand for increased ground water withdrawal, resulting in a subsidence rate of 2.59cm/yr (Al Mukaimi et al., 2018a, and Al Mukaimi et al., 2018b). In addition, increased industry and urban activity, runoff from the chemical plants along the HSC, litter from nearby neighborhoods, have contributed to the elevated contaminants found in the SJE. Large storm events likely eroded the river bed and cause buried contaminants to become re-released and re-distributed into the water column and within the bay sediment. The building of the San Jacinto Dam has also influenced the lower SJE causing a reduction of larger sediment size and freshwater supply to the system, causing an increase in salinity. The stressor cause by both the contaminants as well as the shifts towards higher salinity are evident in the benthic foraminifera record, indicated by number of “stressed” individuals. The building of the San Jacinto Dam has also influenced the lower SJE causing a reduction of larger sediment size and freshwater supply to the system.

Scott Bay and SJE are also subject to regular large storm events like hurricanes that can cause large storm surges and fluxes of freshwater into the river systems that both result in flooding of the area by both freshwater rainfall and brackish storm surge waters. The influence of subsidence, the dam, and salinity

intrusion rise to the system has forced the environment to permanently change from a riverine system to an estuarine system. The benthic foraminifera record provides evidence of the environmental shift from riverine environment, to an estuarine environment, indicated by a shift to a large abundance of saline/brackish favored species (eg. *Ammonia beccari* and *Ammotium salsum)*. The persistent influences of subsidence and loss of sediment supply due to the San Jacinto dam reinforced by the likelihood of storms of increased strength on the system, will continue to drive change in the existing environment going forward.

CHAPTER III: HURRICANE HARVEY'S EFFECT ON EROSION AND DEPOSITION IN SAN JACINTO ESTUARY

3.1: Introduction

The central research objectives of this portion of the project was to determine:

1. how much sediment was eroded,
2. how much new sediment was redistributed and
3. what, if any, shifts are shown in the benthic foraminifera record as a result of the flooding of the San Jacinto River and Buffalo Bayou following Hurricane Harvey.

Assessment of the changes were determined through correlations of down-core sedimentary records between pre- and post-Harvey cores using down core Hg concentrations profiles, grainsize profiles, sediment core x-radiographs, core photographs, and benthic changes in down-core foraminifera assemblage distribution. Through analyses of these parameters the following hypotheses will be either supported or refuted:

H1: *The amount of Hg deposited in SJE, as a result of the erosion of the river bed during Hurricane Harvey, is less than the amount of Hg previously buried within the SJE Hurricane Harvey flood layer.*

H2: *The benthic foraminifera estuarine specific species, as a result of the flux of freshwater from San Jacinto river and Buffalo Bayou floods, will have been eroded from further up stream and redeposited closer to river mouth.*

3.2: Background

Hurricane Harvey

On August 27, 2017, Hurricane Harvey hit the Texas coast and stalled over the Houston area resulting in severe flooding and 80 associated fatalities. This event resulted in unprecedented rainfall, dropping in range of 101.6-155cm in Southeast Texas over the course of four days (The Weather Channel, 2017). The Addicks, Barkers and Lake Houston reservoirs released a combined amount of 0.79×10^9 m^3 of freshwater into Galveston Bay over the course of 2 months (**Figure 12,** Du et al., 2018, in review). The San Jacinto river experienced a peak flood rise of 4.2m of water (USGS, 2017).

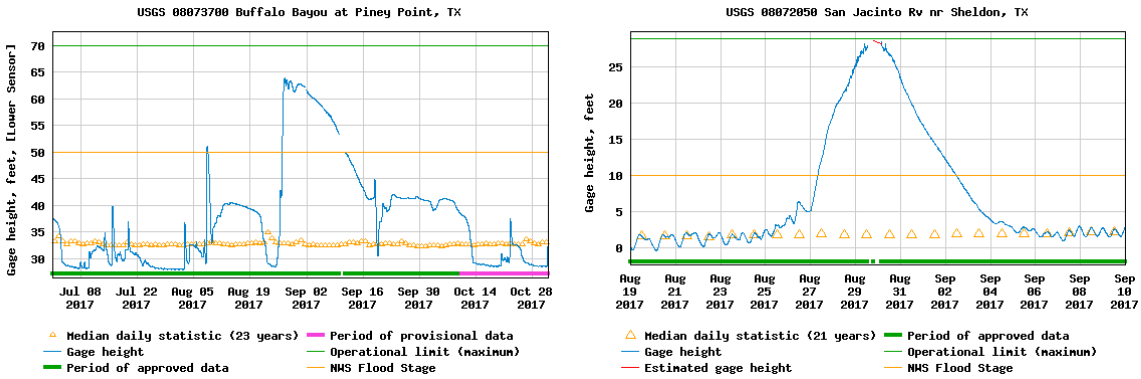

Figure 12: Water gauge readings from USGS of Buffalo Bayou, and San Jacinto River, during and after Hurricane Harvey.

According to FEMA (2017), the flooding impacted more than 100,000 homes in the greater Houston area. Localized subsidence, increases the impact

of events like this away from immediate waterways. Not only do such events result in surface sediment runoff into the river systems, but, due to such a large volume of water, river beds can be eroded, creating a further increased sediment load (and associated contaminant load) to be transported further downstream.

3.3: Methods

Various methods were used to analyze: heavy metal (Hg) contaminant concentration trends, grain size distribution, LOI testing, and benthic foraminifera assemblages. Geochemical methods followed a similar protocol to that described by Nittrouer et al. (1979), and Al Mukaimi et al. (2016). The micropaleontology method is the same as that which was used in chapter 1 of this thesis (Brunner et al., 2013).

3.3.1: Core Collection and Processing

A total of 25 push cores were collected from the lower SJE and Galveston Bay over the course of a a series of day cruises in October through December 2017, beginning eight weeks after the hurricane made landfall. Aluminum core barrels with a diameter of 7.62 cm were extracted, sealed upon recovery and stored in a large freezer at a temperature of 4°C to await processing. In the laboratory, each core section was split lengthwise where one half was to be sampled and the other half preserved intact for archive storage. Digital photographs were taken of each section, with over lapping intervals, images and X-Rays were taken. The post-Harvey cores were sampled only for Hg, and a select few cores sampled for micropaleontology analysis.

Using x-radiographs to identify the storm layer and the pre- Harvey layer, once identified the total storm layer (post-Harvey) was well mixed and so was the total pre-Harvey layer. These two integrated layers were sampled from and used for this portion of this study.

3.3.2: *X-Radiography*

X-Radiographs were acquired for the 2017 post-Hurricane Harvey push cores. Images were acquired using the MinX-Ray HF100+ Amorphous Silicon Imaging System 4030R, X-Ray unit with an energy concentration of 60 kV for an exposure time of 1/20 seconds (Al Mukaimi, 2016).

3.3.3: *Total Mercury (Hg) Analysis*

In order to use a Direct Mercury Analyzer (DMA-80) for the analysis of the total Hg concentration present, samples were dried, and ground into a powder of homogenized sediment. All sample concentrations were put through the test procedure. This required the use of several sample standard tests to be run in addition to the actual sediment samples. This ensured the reliability and consistency of the results due to any loss of Hg as a result of the chemical reactions between the acids in the machine and the nickel boats in which the samples were placed. The standard for this test is the Certified Reference Material (CRM) a MESS-3 (0.091 ± 0.009 ppm) marine sediment standard from the National Research Council of Canada. Among the actual sediment samples and standard samples, a few of the system's sampling boats are left empty as blanks so to make sure there is no cross sample contamination, as well as to ensure

accuracy as the samples go through analysis. Every ten samples for each system run were duplicated to verify result accuracy. A total of 30 sediment samples, 3 blanks, and 6 MESS samples made up each system run (Almukaimi, 2016).

The Direct Mercury Analyzer (DMA-80, milestone srl, Italy) is operated in compliance with the US EPA Method 7473 for the analysis of mercury in solids through thermal decomposition, amalgamation, and atomic absorption spectrophotometry (EPA, 1998). The machine first thermally decomposes the samples in a controlled furnace so as to release the mercury from the sediment. The flow of oxygen through the furnace carries away the decomposition products to a hot catalyst at 615 °C. This reduces the trapped halogens, nitrogen, sulfur oxides and all mercury species to its elemental form. The Hg, in its vapor form, is carried with oxygen to a gold amalgamator for it to be selectively collected. The amalgamator is then heated to 900°C leading to the release of the Hg vapor to be carried away to hot curet cells (125°C) for atomic absorption spectrometry. The Hg is quantified by its absorption at 253.7nm wavelengths which is a function of Hg concentration (Almukaimi, 2016). The standard MESS-3 needs to be within a certified range and average recovery rate of 97 % ± 7 % (Mean ± RSD, n = 137). Results were then exported to Excel.

3.3.4: *Micropaleontology Analysis*

From the several core samples collected 10 cores were selected for Micropaleontological analysis, due to time constraints. In those core samples, the identified storm layers were all integrated and a sample of 1.25-2.5 cm^3

was taken and sieved to preserve grain sizes at >63 μm. The samples were then placed in clean glass beakers to be dried in an oven over night. The benthic foraminifera identified in each sample were then picked and sorted by species into standard 60-box micro paleontological slides. Taxonomy present were identified and counted using a microscope. Where deformed species are found those too will be counted and sorted to species as closely resembling as possible. Severely deformed individuals can be near impossible to identify to the species level.

Morphological attributes of foraminifera tests abnormalities that indicate “stressed” and will be counted as deformed are as follows (Brunner et al., 2013; V. La Cadre and J. Debenay, 2006; Yanko etal., 1994):

1. Change in coiling direction,
2. Change in axis coiling,
3. Misshapen chambers/ protuberances,
4. Multiple apertures,
5. Chamber inflammation,
6. Conjoined twinning, and
7. Deterioration of tests

Benthic foraminifera deformations and taxa of each sediment layer were compared to the Hg results and the storm deposit thickness, in order to be considered against the study hypotheses.

3.3.5: *Geographical Information Systems (GIS)*

Several maps of the distribution of storm layer thickness, hg concentrations, and benthic foraminifera assemblage distribution, were created in order to understand geographically, how SJE sediments and benthic foraminifera communities were affected by Hurricane Harvey's large flux of freshwater through the system.

3.4: Results

3.4.1: Hurricane Harvey Sediment Deposit

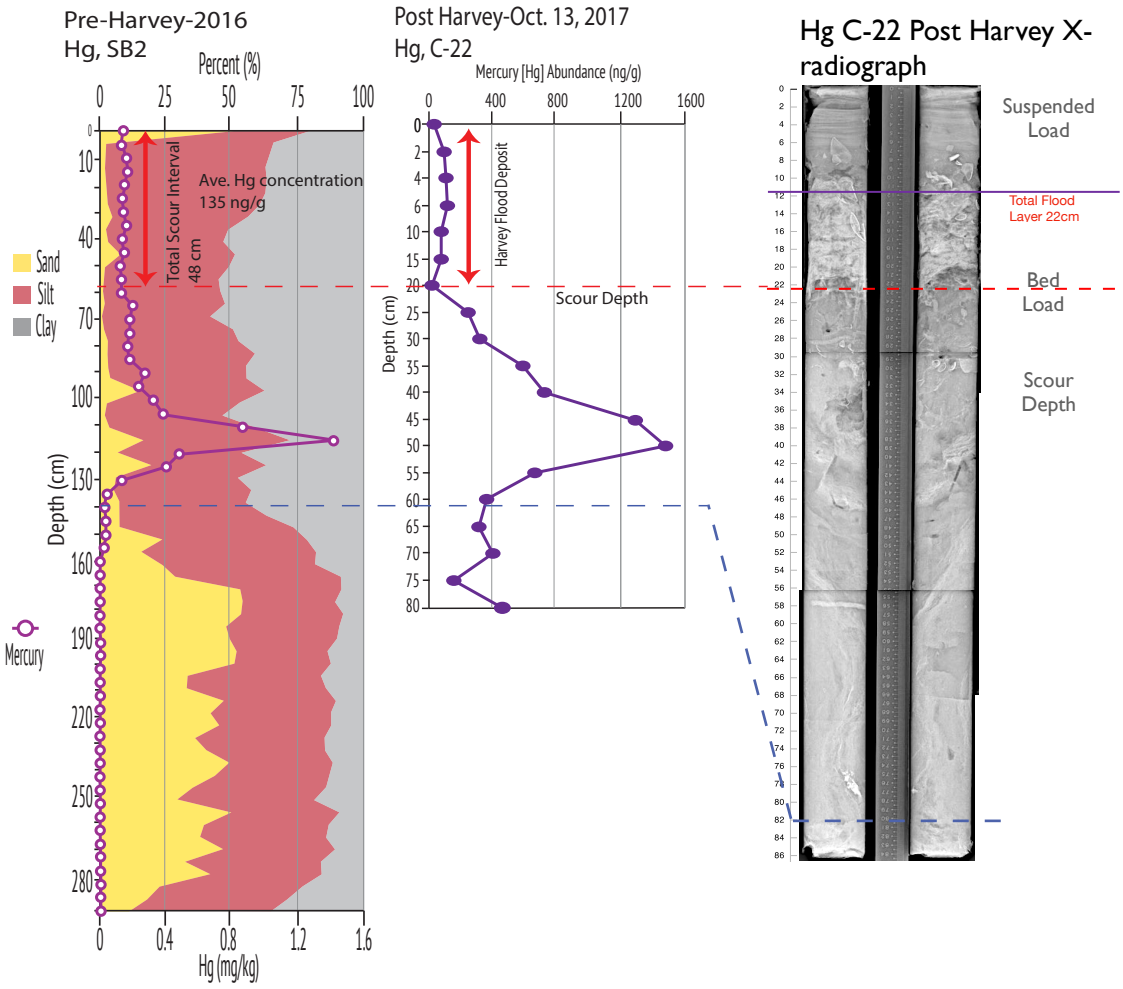

Figure 13: Pre-Hurricane Harvey core SB1 compared to Post-Hurricane Harvey core C-22, from Scott Bay, Hg profile, x-ray mosaics (right), depicting Pre-and Post Harvey deposition. Post-Hurricane Harvey core collected November 2017, 8 weeks after storm landfall.

In Post-Harvey Core 22, (**Figure 13**) the x-radiograph reveals the presence of a 22 cm thick layer at the surface of the core. The base of this new layer is marked by an erosional layer and a 14 cm thick basal deposit consisting of shell

gravel and sand. The shells included intact shells up to 2-3 cm long and coarse shell fragments as well as shell gravel. There is a sharp transition at 4 cm in the core, above which there is a layer of well laminated mud, with sandy laminations, the average sand content of this interval is 25%. This upper 22 cm thick layer found in post-Hurricane Harvey Core 22 is interpreted as the Hurricane Harvey layer, with the coarse basal portion of the flood layer represents the bed load transported during the higher flow conditions and the finer upper layer having

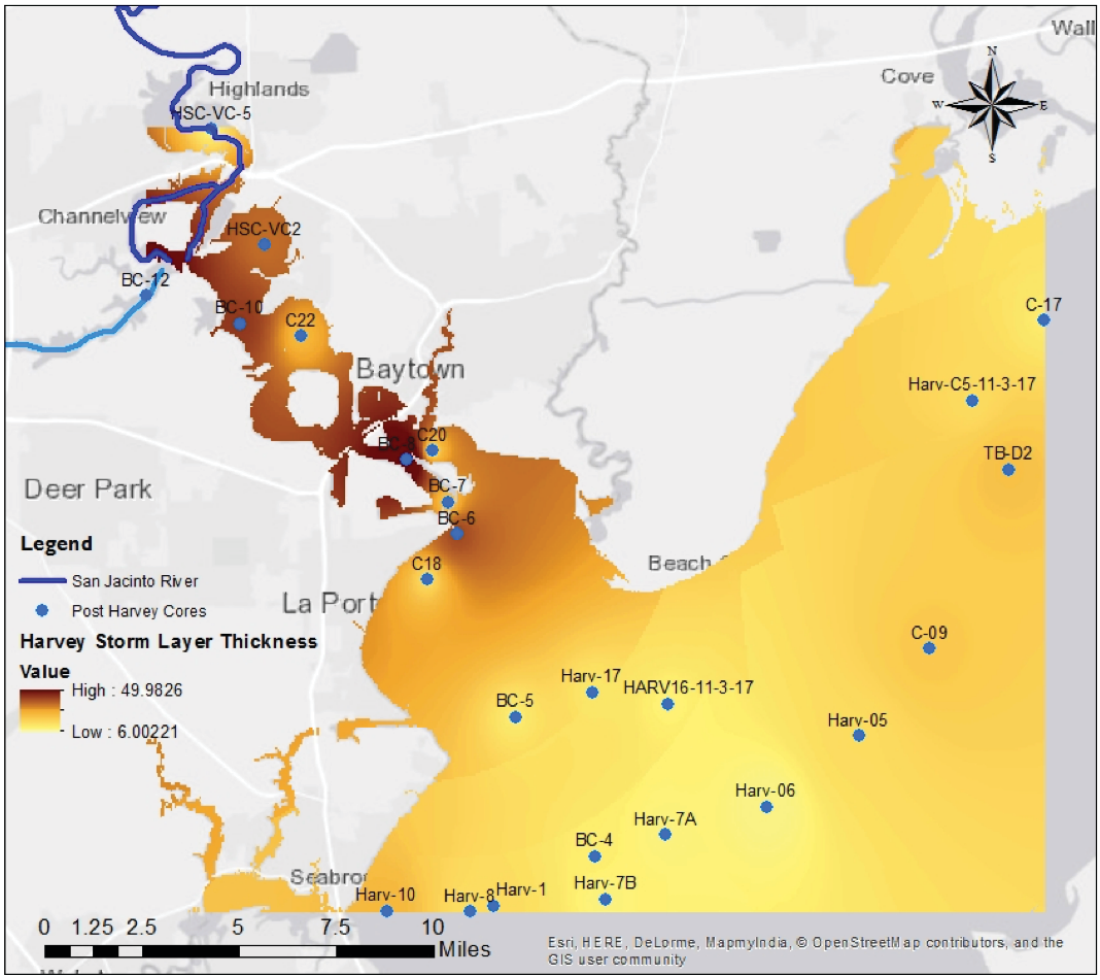

Figure 14: Post-Hurricane Harvey storm deposit thickness. GIS map of each core storm thickness distribution in the lower San Jacinto Estuary, spatially interpolated using ArcGIS. Post-Hurricane Harvey cores collected November 2017, 8 weeks after landfall.

been deposited during the waning phase of the flood, and represents deposition of the suspended load post flood surge clay deposit approximately 44 days later. With these layers clearly identified in each of the Post-Harvey cores, each core thickness was then spatially represented for comparisons (**Figure 14-20**).

In **Figure 14** the Hurricane Harvey sediment deposit is seen to be thickest in the semi enclosed bays of the HSC and thins out closer to the more open Galveston Bay. A storm deposit of maximum 50cm thickness was found deposited in these semi enclosed bays, and the thinnest of 6cm thickness in the Galveston Bay cores.

3.4.2: *Pre vs. Post Hurricane Mercury Concentrations*

Using the integrated post-harvey sample and the integrated pre-Harvey samples for Hg concentration analysis, the results were then spatially graphed using ArcGIS (**Figure 15 & 16**). In the pre-Harvey sample laters high Hg concentrations, were found to be in the HSC and Scott Bay area, with concentrations as high as 157 ng/g and a low of 14.5 ng/g at the opening into Galveston Bay (**Figure 15**). In the cores collected 8 weeks after the Hurricane Harvey made landfall, the surface Hg concentrations had changed. Within the newly deposited sediment load, the highest Hg concentrations, indicated from these cores, were found in the Scott Bay area of HSC, the concentrations didn't change much from 157 ng/g (Pre, **Figure 15**) to 154 ng/g (Post, **Figure 16**). Closer to the opening into Galveston Bay and in the Bay itself, the Hg concentrations had significantly decreased to as low as 0.004 ng/g.

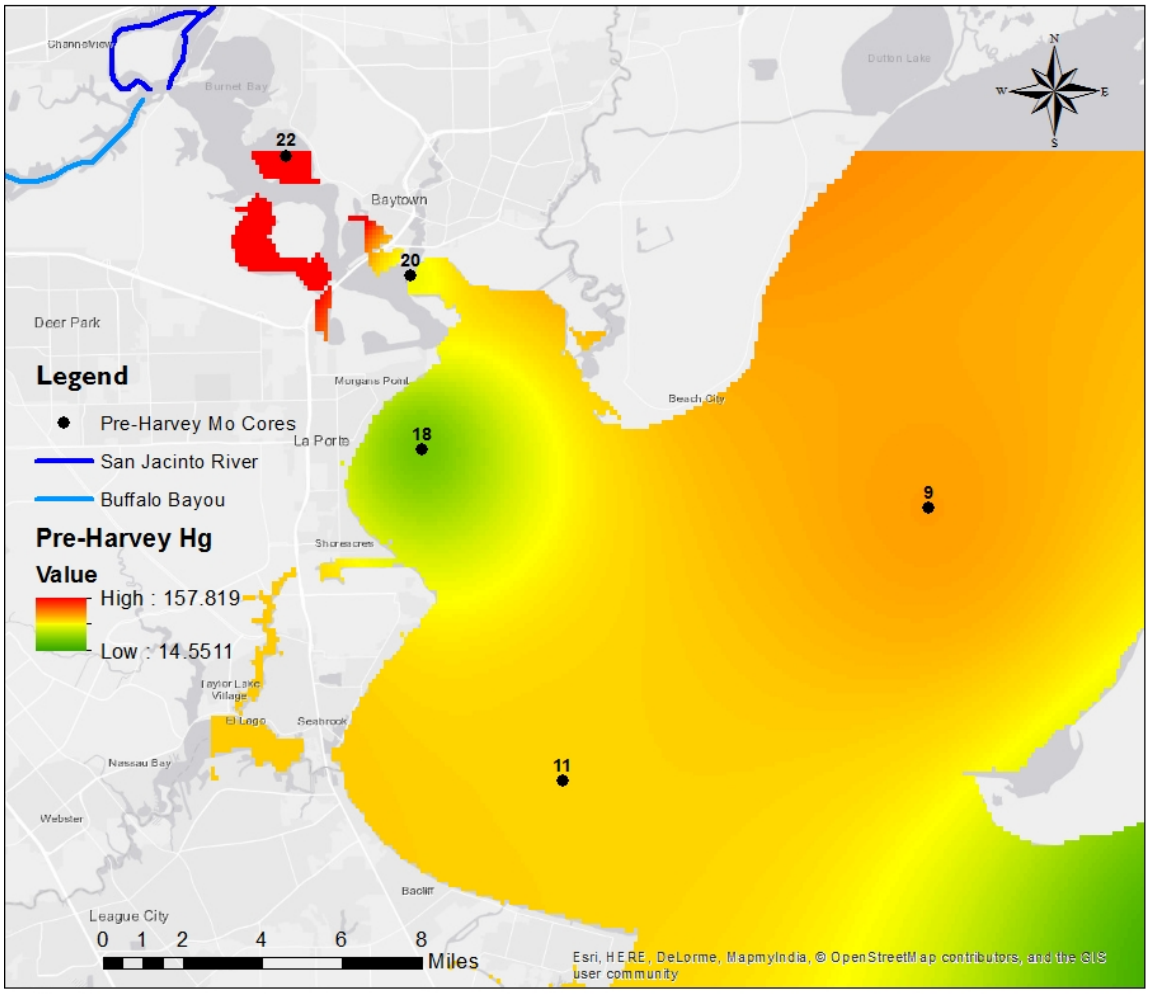

Figure 15: Pre- Hurricane Harvey Hg surface concentration, spatially interpolated using ArcGIS. Pre-Harvey core data collected in 2012 from previous study (Al Mukaimi et al., 2018a, and Al Mukaimi et al., 2018b).

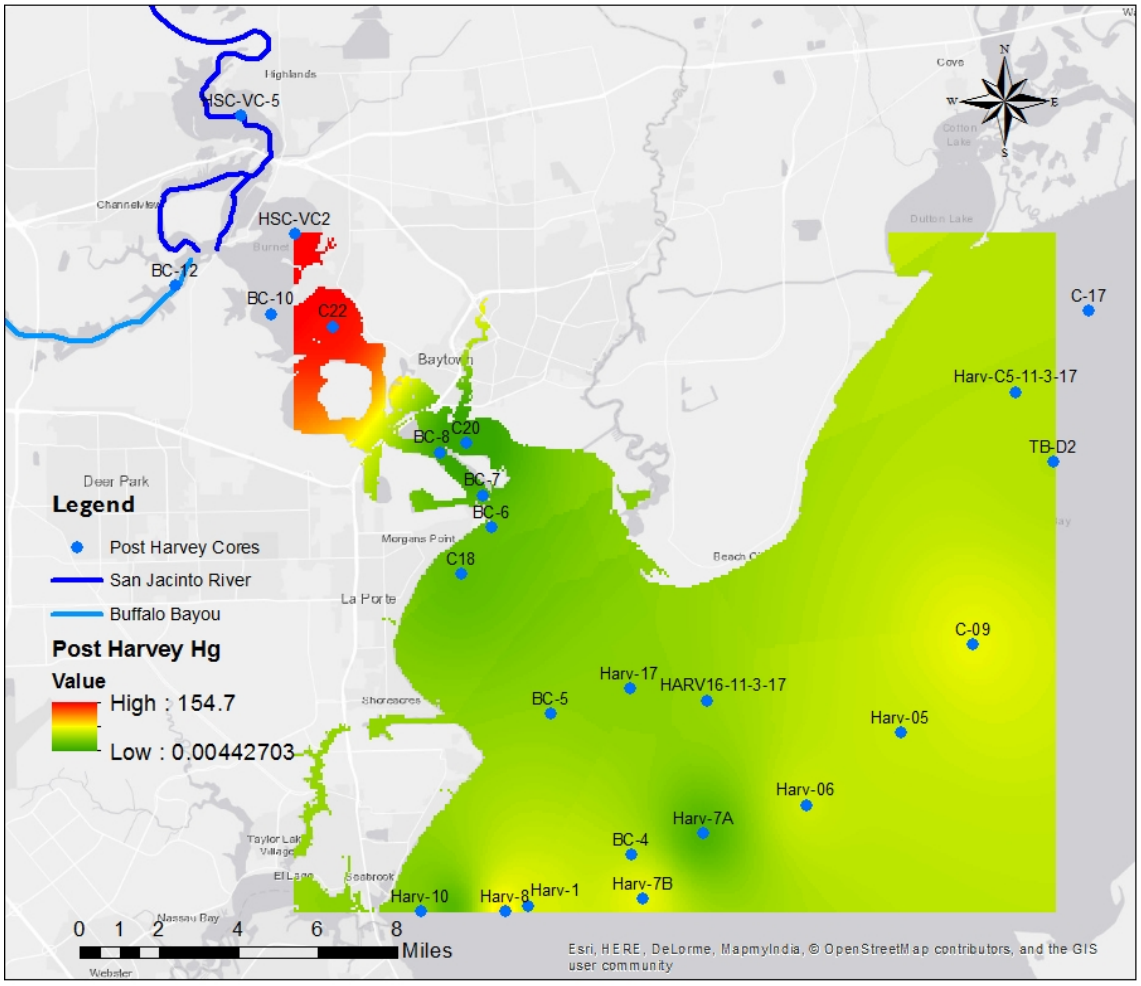

Figure 16: Post- Hurricane Harvey Hg surface concentration, spatially interpolated using ArcGIS. Pre-Harvey core samples collected November 2017, 8 weeks after Hurricane Harvey landfall.

3.4.3: *Hurricane Harvey's Effects on Benthic Foraminifera*

From each Post-Hurricane Harvey core, surface samples were collected and analyzed for benthic foraminifera. **Figures 17-20** depict the abundance of various species mapped spatially in ArcGIS, in the lower SJE and upper Galveston Bay. Note, there are a series of dredge spoil islands at the head that extend southward from the northern shoreline, separating Trinity and Galveston Bay, with the dredge navigation channel extending down the western side of the

island, effectively isolating the effluent from the SJE to Galveston Bay and restricting the advection of its flow into Trinity Bay. The total species abundance observed is greatest in Galveston Bay, particularly in core HARV7A with a count of 3098 individuals, and a low abundance was observed near the HSC with 117 individuals in core C22 (**Figure 17**). Core HARV16 was collected 14.2 km south of the mouth of the San Jacinto River and had a total individuals count that was relatively low, with a count of 14 individuals. In contrast, Core HARV7A is located

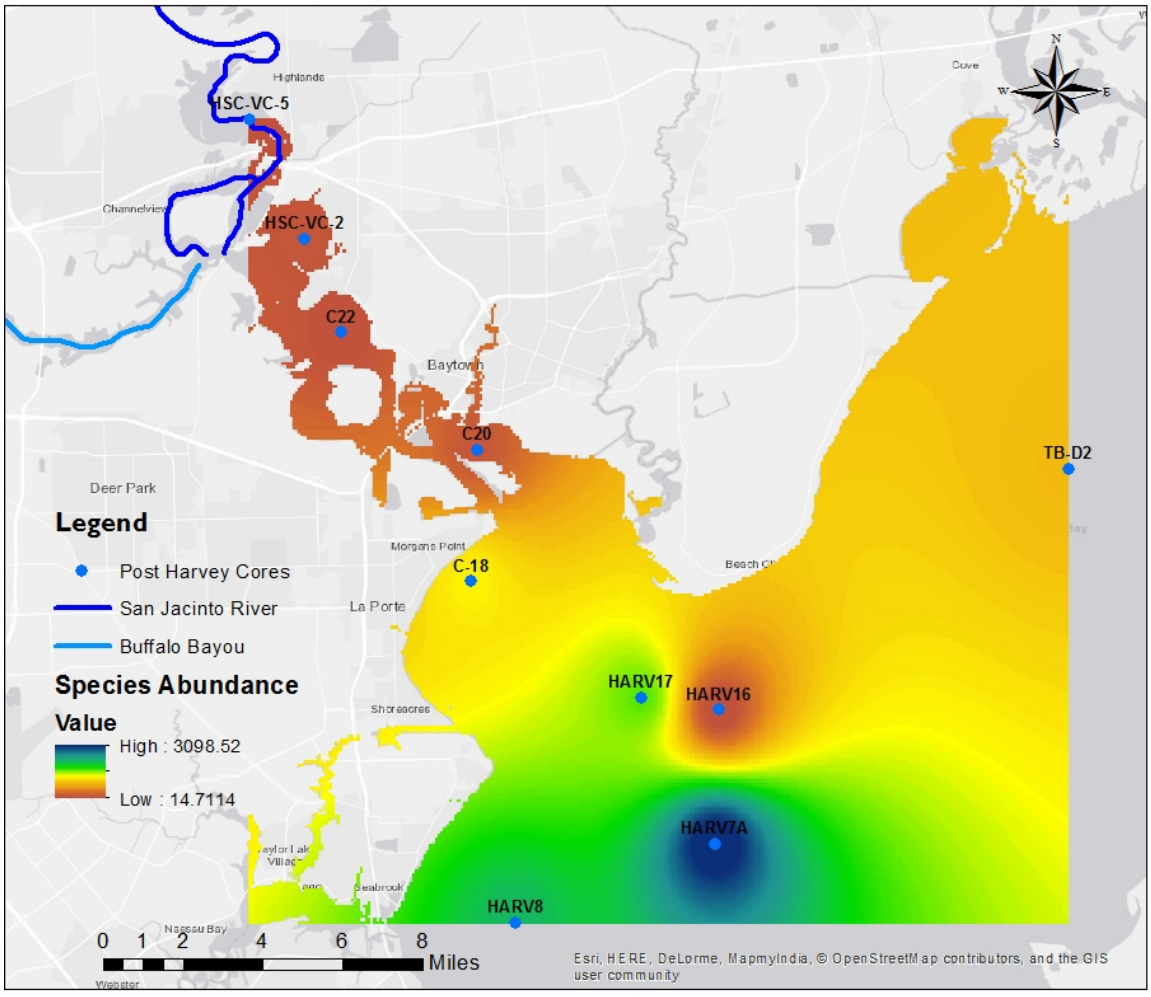

Figure 17: Post- Hurricane Harvey benthic foraminifera Total Species Individual abundance, spatially interpolated using ArcGIS. Post-Hurricane Harvey cores collected November 2017, 8 weeks after landfall.

only 4.5 km down the bay from Core Harv 16, but contained the highest abundance of 2337 Ammonia beccari specimens, while HARV16 contained the least amount of only 1 specimen. The core furthest south, HARV8, has a count of 2147 individuals, where as further north in Trinity Bay, core TB-D2 had a smaller count of 869.

The spatial distribution of the *Ammonia beccari*, a brackish environment dominating species, was found to be similar to the total individual abundance

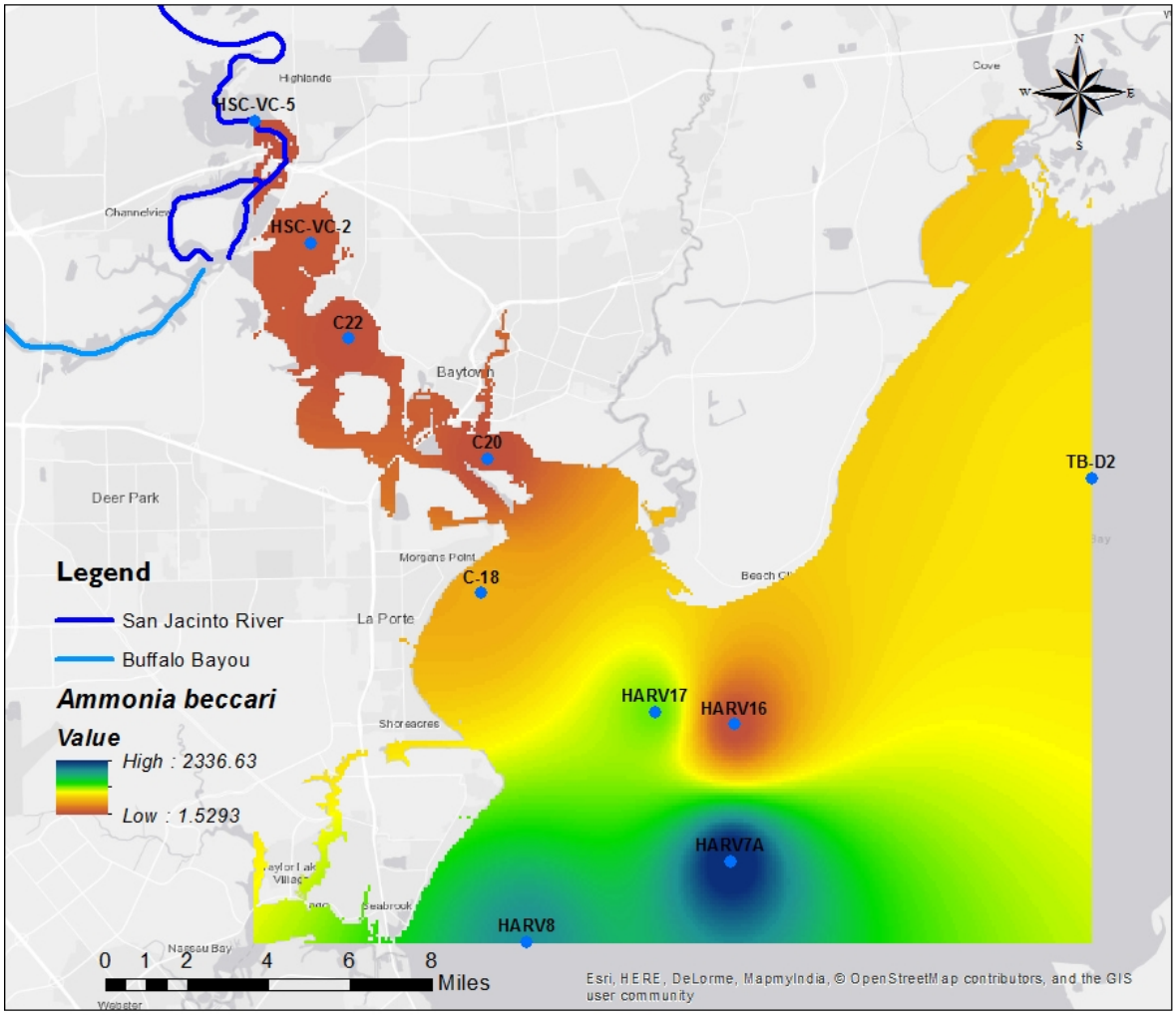

Figure 18: Post-Hurricane Harvey benthic foraminifera *Ammonia beccari* species counts, spatially interpolated using ArcGIS. Post-Harvey core samples collected November 2017, 8 weeks after Hurricane Harvey landfall.

distribution. (**Figure 18**). Core HARV7A contained the highest abundance of 2337 *Ammonia beccari* specimens, while HARV16 contained the least amount of only 1 specimen. Cores, C22 and VC-2, both from the SJE, contained a low species standing stock of about 117 and 153, respectively.

Looking at **Figure 19**, the species of foraminifera, *Elphidium sp*., that is capable of adapting and quickly recolonizing harsher environments was only abundant in core HARV7A, with a standing stock of 287. In the HARV16 core

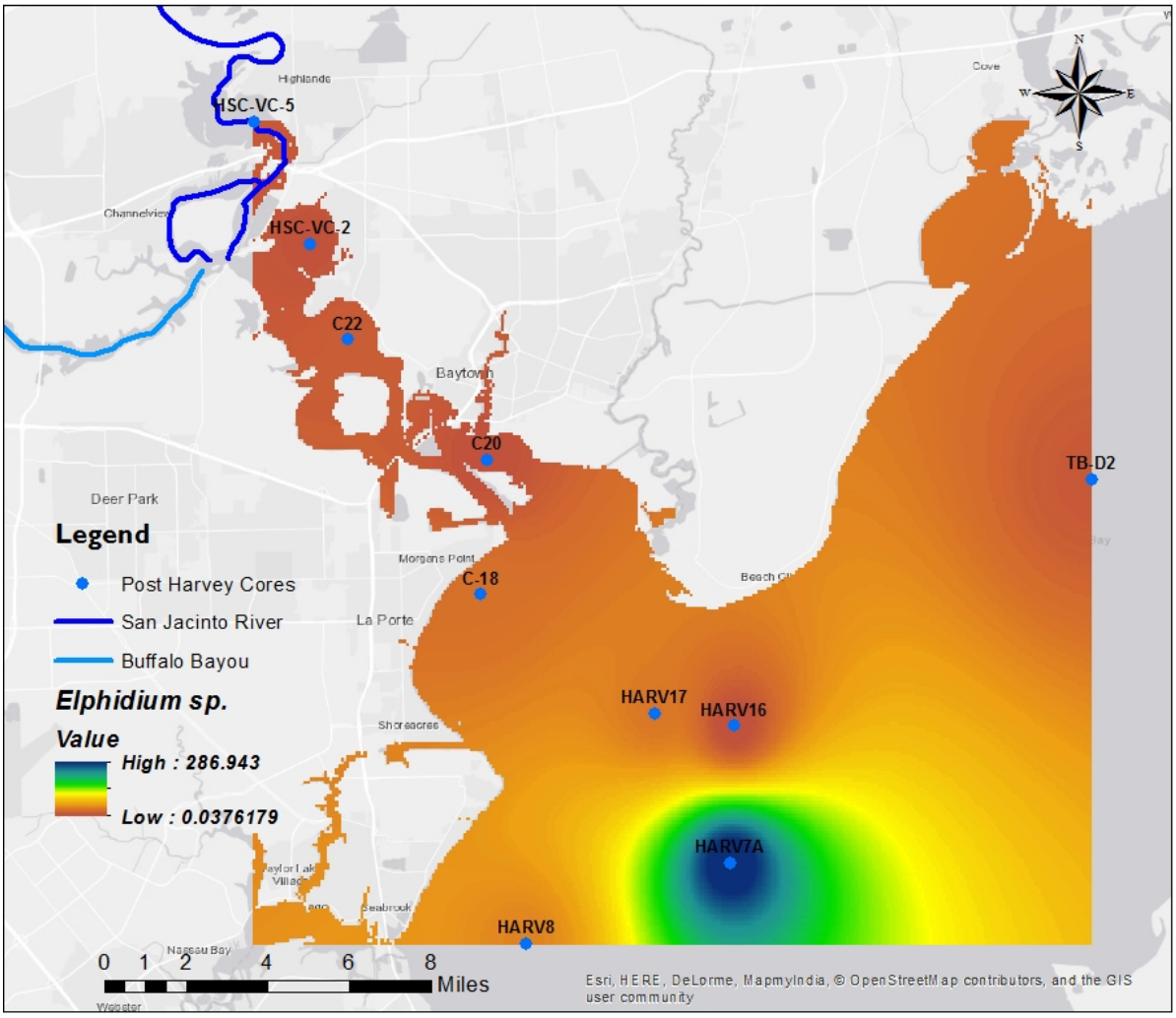

Figure 19: Post- Hurricane Harvey benthic foraminifera *Elphidium sp.* species counts, spatially interpolated using ArcGIS. Pre-Harvey core samples collected November 2017, 8 weeks after Hurricane Harvey landfall.

there were 0 specimens of *Elphidium sp*. found, whereas the other two cores in close proximity, HARV8 and HARV17, had a standing stock of 43 and 39, respectively. The HSC cores of C22 and VC-2 also had a low standing stock of 16 and 7 *Elphidium sp.* individuals.

In **Figure 20** *Miliamina fusca* species, typically found in bay head deltas (Poe et al., 2016) showed an interesting abundance distribution. The individual count of *Miliamina fusca* was found to be increasing further south towards the

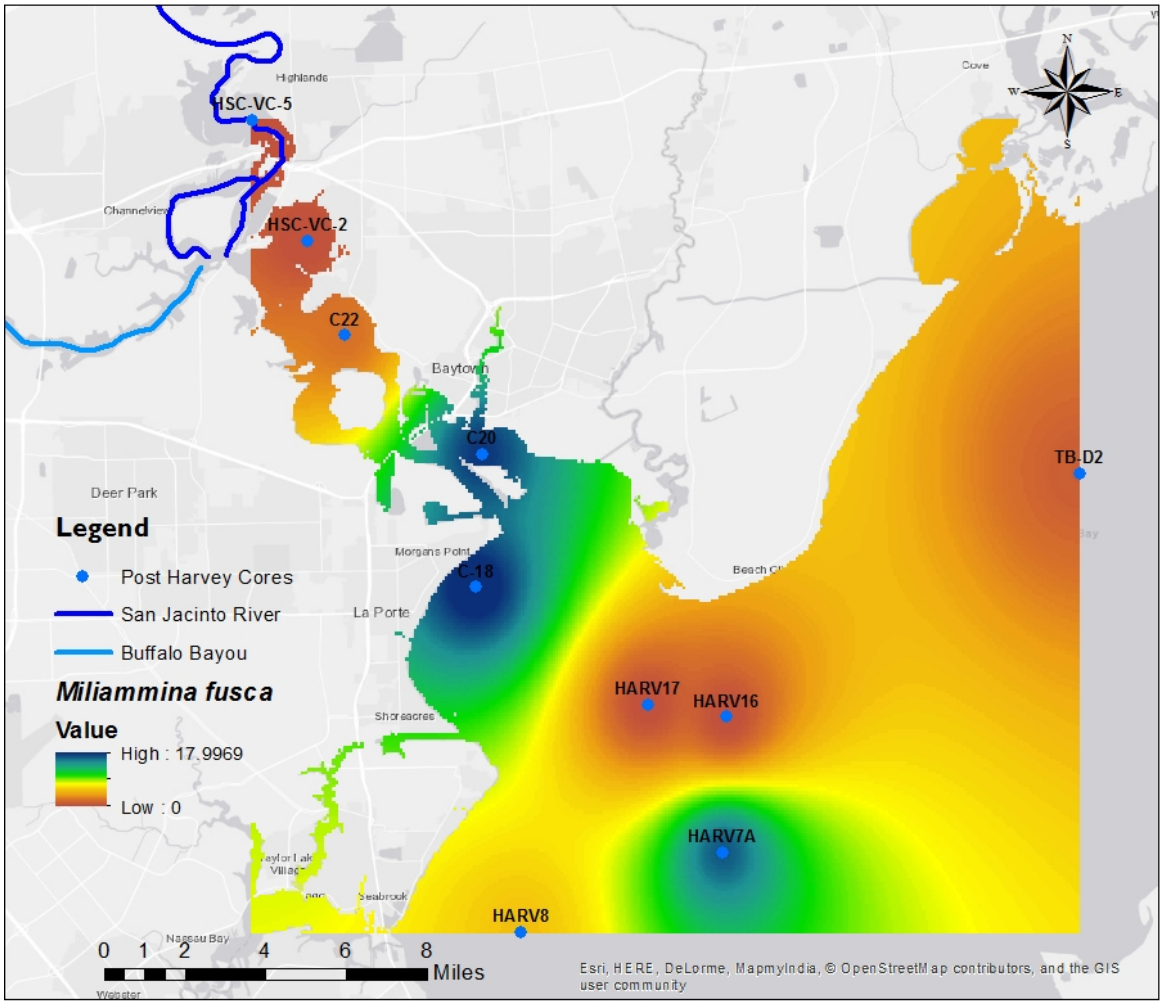

Figure 20: Post- Hurricane Harvey benthic foraminifera *Miliammina fusca* species counts, spatially interpolated using ArcGIS. Pre-Harvey core samples collected November 2017, 8 weeks after Hurricane Harvey landfall.

opening to Galveston Bay, and then decreasing at and beyond the Bay opening. The two cores furthest up stream in the HSC, C22 and VC-2 had a standing stock of 2 and 0 individuals, respectively. However, in core C20, at the opening to Galveston Bay, there was a larger standing stock of 17 individuals. Core C18, in close proximity to C20, also had a similar count of 18 individuals. Further out in Galveston Bay, HARV7 had a high count of 16 individuals but HARV17 and HARV16, both relatively close to HARV7, to the south, and C18, to the northeast, both had 0 *Miliammina fascia* species present (**Figure 20**).

3.5: Discussion

3.5.1: Sediment and Mercury Redistribution

The vast amount of floodwater that flowed into the SJE from Buffalo Bayou and the SJR caused extensive seabed erosion of the SJE, including Scott Bay. Observations from the Core 22 site found that 48 cm of sediment had been eroded from the site and 22 cm of flood derived sediment was deposited to partially replace the eroded sediment (**Figure 13**). The flood deposit included 12 cm of basal sand deposit representing the bedload and 10 cm of mud representing the suspended load. The storm sediment deposits were identified to have been mainly trapped in smaller semi enclosed embayments as seen in **Figure 15**. The sediment eroded by Hurricane Harvey at the Core 22 site contained elevated Hg concentrations averaging 125 ng/g, whereas the Harvey deposits deposited atop the erosional surface has concentrations averaging 80 ng/g.

The erosional surface within the x-radiograph (**Figure 13**) at the base of the flood layer suggest that there was erosion of the bed during the peak flood discharge conditions. The Hg enriched SJE sediment eroded by Hurricane Harvey was flushed into Galveston Bay and some of it was incorporated into the Hurricane Harvey flood deposit found within the bay (**Figure 14** and **16**). This supported the H1 hypothesis; that Hurricane Harvey's flood currents eroded the previously buried Hg content redistributing it back into the water column, during

the storm, and flushed the highly contaminated flood waters out through Galveston Bay, leaving behind a lower surface Hg deposit.

3.5.2: *Sediment Deposit vs. Foraminifera Abundance*

Comparing the estuarine species of ***Ammonia beccari*** and ***Elphidium sp.*** that were found in the surface sample of pre-Hurricane Harvey in Scott Bay were absent in the post Hurricane Harvey integrated storm layer samples collected in 2017. This indicates the H2 hypothesis is supported and that the large flux of fresh water from the storm surge eroded those bottom sediments and transported the sediment containing these benthic foraminifera communities that were present in the pre-Harvey deposits out to the upper Galveston Bay. This created a decrease in abundance proximal to the river mouth.

The species of ***Miliamina fusca*** that is characterized by Poeg (2015) as a "river bay head delta" species, was found in abundance at the opening of the SJE to Galveston Bay, providing evidence that a portion of the sediment eroded in Scotts Bay and likely the areas downstream of the confluence of the SJE and Buffalo Bayou was deposited in the areas where there are elevated ***Miliamina fusca*** counts as shown in **Figure 20**. This area also contains elevated Hg concentrations, consistent with the transport of Hg enriched sediment and the sediments from Scotts Bay that were eroded by Hurricane Harvey were also enriched in Hg.

An alternative explanation could be that, due to the large flux of fresh water eroding the sediment bed, from Buffalo Bayou and San Jacinto River during the

44 days of flooding, the *Miliamina fusca* specimens found at the bottom of the SJE near the opening to Galveston Bay, is a reflection of how far up stream sediment was eroded and transported from where they lived previously to where they were deposited. Given that according to V. La Cadre and J. Debenay (2006), foraminifera under stressful conditions may take between 15-30 days to asexually reproduce but delay their initial chamber construction from previously being 20 days to now 37 days and take an additional 5-7 months for full growth. So within the 8 weeks from flood event to sample collections, the foraminifera would not have been able to have been far enough along in their growth cycle in order to reflect the newly changed environment.

Having collected the post-Hurricane Harvey cores only eight weeks after landfall and three weeks after river flooding subsided, the semi closed bays in proximity to the river head may not have recovered enough from the flux of freshwater to allow for the estuarine species to return. New surface samples would need to be collected to prove both the recovery of saline specific species and the shift of Bay head delta back to its pre-storm location, but this is beyond the scope of this project.

2.6: Conclusion

Hurricane Harvey forced flood waters of about 11.1×10^9 m of freshwater into the Galveston Bay area over the course of 2 months, and delivered about 9.86×10^7 metric tons of sediment (Du et al., 2019). The freshwater inflow into the system was 3 times the volume of the Bay and therefore completely refreshed

Galveston Bay for over two months. Using multiple push cores collected eight weeks after the storm made landfall, the analysis of Hg showed that, at the Core 22 site, 48 cm of bottom sediments were eroded causing buried contaminants to be reintroduced to the water column and flow downstream in to the Bay.

Post Harvey cores have also provided evidence that the benthic foraminifera from the surface samples had been eroded from sediment banks further up stream of the Buffalo Bayou and the San Jacinto River and then transported to Galveston Bay. With the integrated storm layer sample it is difficult to definitively conclude where the source of the deposited sediment was eroded from. The decreased standing stock of the brackish foraminifera species, *Ammonia beccari*, and *Elphidium sp*. is characteristic of a low salinity environment but the species did not have enough time in those 8 weeks to repopulate in their preferred environment setting and so we were too early in our sampling to be able to capture the changed environment. According to Du et al. (2019), the Bay salinity did not recover to pre-storm concentration for another two months after the storm. If more surface samples were to be taken now, it may be possible to see evidence that species abundance has returned to prior storm concentrations.

CHAPTER IV: STUDY CONCLUSIONS

In the studies presented here, anthropogenic and environmental influences were investigated in the lower San Jacinto Estuary. The first study focused on the historical anthropogenic affects identifiable in the sedimentary record and how it has changed the environment of the SJE. The core samples collected in 2016 provided evidence towards Chapter I: The Environmental and Pollution Geologic Record from Past Century in Scott Bay, and the following hypotheses:

H1: *Historic events like that of the building of San Jacinto Dam and large hurricanes/storms will be indicated by a decrease in sand or clay deposits, respectively*.

H2: *The increase in urbanization around Scott Bay will indicate an increase in mercury (Hg) concentration and therefore cause the benthic foraminifera to show indication of stress.*

H3: *The installation of the dam caused a reduction in both freshwater and sediment input. As a result, Scott Bay became deeper, and the saltwedge migrated upstream. This is reflected in the sediment record as a shift from freshwater to brackish benthic foraminifera species.*

The H1 hypothesis was supported by finding a correlation between a reduction of sand deposits from the building of the San Jacinto Dam, and a few clear signals were found correlating to historical Hurricane storm events. The H2 hypothesis was supported due to the increased abundance of “stressed” benthic

foraminifera individuals correlating with the prominent Hg peaks identified in core SB1 and with the San Jacinto Dam construction in 1953 a reduction in freshwater and sediment supply wouldn't have been able to prevent a buildup of contaminants. The H3 hypothesis was supported by the benthic foraminifera record indicating a change from no saline/brackish, therefore riverine environment, specific species below 100cm, down core, to the estuarine environment species, like that of ***Ammonia beccari,*** becoming the dominant species in the Scott Bay and lower SJE region.

The second study analyzed the impact of Hurricane Harvey on the estuary system and Galveston Bay. The core samples collected eight weeks after Hurricane Harvey which made landfall in August 2017, provided evidence towards Chapter II: Hurricane Harvey's Effect on Erosion and Deposition in San Jacinto Estuary, to assess hypotheses:

H1: *The amount of Hg deposited in SJE, as a result of the erosion of the river bed during Hurricane Harvey, is less than the amount of Hg previously buried within the SJE Hurricane Harvey flood layer.*

H2: *The benthic foraminifera estuarine specific species, as a result from the flux of freshwater from San Jacinto river and Buffalo Bayou flooding during Hurricane Harvey, will show a decrease in abundance closer to river mouth.*

The H1 hypothesis was supported through the comparison of pre-Harvey Hg concentrations being higher than that of the Post-Harvey Hg concentrations. The H2 hypothesis was also supported by the benthic foraminifera record

showing that the influx of sediment derived from freshwater areas from SJR and Buffalo Bayou were deposited in Scott Bay resulting in a decrease in brackish specific species.

This thesis shows that the lower SJR estuary has been impacted both by the input of anthropogenic pollutants released into the environment from the industrial activity, as well as the reduction in freshwater and sediment input due to the construction of the San Jacinto Dam, as well as by significant storm events, including both storm surges and river flooding. These impacts have collectively and individually (e.g. Harvey), caused the system environmental shift reflected in the foraminifera communities found with the sediment as well as the redistribution of previously buried pollutants found within the sediment.

4.1 Further Considerations

This study shows what kind of impacts the local industry has had on the San Jacinto Estuarine meiofaunal community, as indicated by the benthic foraminifera record. A large amount of buried pollutants were reported in Chapter 2, and it was shown that these legacy pollutants can be eroded and redistributed into the water column. During and post Hurricane Harvey land fall, there was a colossal volume of flood water caused by the Buffalo Bayou, and San Jacinto River transporting the eroded sediment, the buried foraminifera, as well as these legacy contaminants into Galveston Bay. The housing communities that are in

close proximity to the HSC became significantly flooded, both up and downstream. After this study, we now know to what extent mercury was redistributed into the flood waters and moved downstream. These contaminants possibly flooded into nearby communities and into close contact with the residence trying to flee the rising waters. To confirm this, core samples from onshore in communities that were flooded during Hurricane Harvey should be collected and analyzed for a greater understanding of how those communities were possibly affected by the redistributed buried contaminants.

Not only large storms or hurricanes can erode and redistribute buried pollutants but construction activities like dredging could possibly disturb highly contaminated sediment. **Figure 4** depicts a very significant spike of mercury content about 90cm down core, if there are other locations around the HSC that contains similar high concentrations buried legacy contaminants, dredging plans could release the contaminants back into the water column. Knowing this, Environmental Project Managers will need to begin to put potential buried contents into consideration for the impact of the execution of their projects.

REFERENCE CITED

Al Mukaimi, M. E., Dellapenna, T., & Williams, J. R. (2016, February). Geochemical and Sedimentary Record of Urbanization and Industrialization of the Galveston Bay Watershed. In ***American Geophysical Union, Ocean Sciences Meeting 2016****, abstract# MG44B-1983*.

Al Mukaimi, M. E., Kaiser, K., Williams, J. R., Dellapenna, T. M., Louchouarn, P., & Santschi, P. H. (2018a). Centennial record of anthropogenic impacts in Galveston Bay: Evidence from trace metals (Hg, Pb, Ni, Zn) and lignin oxidation products. ***Environmental Pollution***, *237*, 887-899.

Al Mukaimi, M. E., Dellapenna, T. M., & Williams, J. R. (2018b). Enhanced land subsidence in Galveston Bay, Texas: Interaction between sediment accumulation rates and relative sea concentration rise. ***Estuarine, Coastal and Shelf Science***, *207*, 183-193.

Alve, E. (1991). Benthic foraminifera in sediment cores reflecting heavy metal pollution in Sorfjord, western Norway. ***Journal of Foraminiferal Research***, 21(1), 1-19.

Alve, E. (1995). Benthic foraminiferal responses to estuarine pollution: a review. ***Journal of Foraminiferal Research***, 25(3), 190-203.

Alve, E. (1999). Colonization of new habitats by benthic foraminifera: a review. ***Earth-Science Reviews***, 46(1), 167-185.

Alve, E., & Olsgard, F. (1999). Benthic foraminiferal colonization in experiments with copper-contaminated sediments. ***Journal of Foraminiferal Research***, 29(3), 186-195.

Alve, E., Lepland, A., Magnusson, J., & Backer-Owe, K. (2009). Monitoring strategies for re-establishment of ecological reference conditions: possibilities and limitations. ***Marine Pollution Bulletin***, 59(8), 297-310.

Alve, E., & Goldstein, S. T. (2010). Dispersal, survival and delayed growth of benthic foraminiferal propagules. ***Journal of Sea Research***, 63(1), 36-51.

Du Chatelet, E. A., Debenay, J. P., & Soulard, R. (2004). Foraminiferal proxies for pollution monitoring in moderately polluted harbors. ***Environmental pollution***, 127(1), 27-40.

Bank, M. S. (Ed.). (2012). Mercury in the environment: pattern and process. University of California Press.

Breard, S., Callender, A., Denne, R., & Nault, M. (2000). "Taxonomic Uniformitarianism in Gulf of Mexico Basin Cenozoic Foraminiferal Paleoecology: Is the Present Always the Key to the Past?" Gulf Coast Association of Geological Societies Transactions, 50, 725-736.

Boltovskoy, E. (1965). Twilight of foraminiferology. ***Journal of Paleontology***, 383-390.

Boltovskoy, E., & Wright, R. (1976). The Systematic Position and Importance of the Foraminifera. In Recent Foraminifera (pp. 1-3). Springer Netherlands.

Boltovskoy, E., Scott, D. B., & Medioli, F. S. (1991). Morphological variations of benthic foraminiferal tests in response to changes in ecological parameters: a review. **Journal of Paleontology**, 65(2), 175-185.

Brunner, C. A., Yeager, K. M., Hatch, R., Simpson, S., Keim, J., Briggs, K. B., & Louchouarn, P. (2013). Effects of oil from the 2010 Macondo well blowout on marsh foraminifera of Mississippi and Louisiana, USA. ***Environmental science & technology***, 47(16), 9115-9123.

Byun, D. S., Wang, X. H., & Holloway, P. E. (2004). Tidal characteristic adjustment due to dyke and seawall construction in the Mokpo Coastal Zone, Korea. ***Estuarine, Coastal and Shelf Science***, 59(2), 185-196.

Centers for Disease Control and Prevention (CDC). (2017, January 26). Lead Infographic. Retrieved January 26, 2018, from https://www.cdc.gov/nceh/lead/infographic.htm

Clampet. A. P. (2012). Methylmercury: formation, sources and health effects. Nova Science Publishers.

Coccioni, R. (2000). Benthic foraminifera as bioindicators of heavy metal pollution. Environmental micropaleontology: the application of microfossils to environmental geology. ***Kluwer Academic/Plenum Publishers***, New York, 71-103.

Coccioni, R., & Marsili, A. (2005). Monitoring in polluted transitional marine environments using foraminifera as bioindicators: a case study from the Venice Lagoon(Italy). ICAM Dossier, (3), 250-256.

Coplin, L. S., & Galloway, D. (1999). Houston-Galveston, Texas. Land subsidence in the United States: US Geological Survey Circular, 1182, 35-48.

Galloway, D. L., Jones, D. R., & Ingebritsen, S. E. (1999). Land subsidence in the United States (Vol. 1182). US Geological Survey.

Corliss, B. H. (1991). Morphology and microhabitat preferences of benthic foraminifera from the northwest Atlantic Ocean. ***Marine micropaleontology***, 17(3-4), 195-236.

Corliss, B. H., & van Weering, T. C. (1993). Living (stained) benthic foraminifera within surficial sediments of the Skagerrak. ***Marine Geology***, 111(3-4), 323-335.

Dabbous, S. A., & Scott, D. B. (2012). Short-term monitoring of Halifax Harbour (Nova Scotia, Canada) pollution remediation using benthonic foraminifera as proxies. ***Journal of Foraminiferal Research***, 42(3), 187-205.

Debenay, J. P., Geslin, E., Eichler, B. B., Duleba, W., Sylvestre, F., & Eichler, P. (2001). Foraminiferal assemblages in a hypersaline lagoon, Araruama (RJ) Brazil. ***Journal of Foraminiferal Research***, 31(2), 133-151.

Debenay, J. P., Millet, B., & Angelidis, M. O. (2005). Relationships between foraminiferal assemblages and hydrodynamics in the Gulf of Kalloni, Greece. ***Journal of foraminiferal Research***, 35(4), 327-343.

Dellapenna, T. M., Kuehl, S. A., & Schaffner, L. C. (1998). Sea-bed mixing and particle residence times in biologically and physically dominated estuarine

systems: a comparison of lower Chesapeake Bay and the York River subestuary. ***Estuarine, Coastal and Shelf Science***, *46*(6), 777-795.

Dellapenna, T. M., Kuehl, S. A., & Schaffner, L. C. (2003). Ephemeral deposition, seabed mixing and fine-scale strata formation in the York River estuary, Chesapeake Bay. ***Estuarine, Coastal and Shelf Science***, *58*(3), 621-643.

Dijkstra, N., Junttila, J., Skirbekk, K., Carroll, J., Husum, K., & Hald, M. (2017). Benthic foraminifera as bio-indicators of chemical and physical stressors in Hammerfest harbor (Northern Norway). Marine pollution bulletin, 114(1), 384-396.

Dolven, J.K., Alve, E., Rygg, B., Magnusson, J., (2013). Defining past ecological status and in situ reference conditions using benthic foraminifera: a case study from the Oslo fjord, Norway. Ecol. Indic. 29, 219–233.

Du Chatelet, E. A., Debenay, J. P., & Soulard, R. (2004). Foraminiferal proxies for pollution monitoring in moderately polluted harbors. ***Environmental pollution***, 127(1), 27-40.

Du, J., Park, K., & Dellapenna, T. M. (2019) Estuarine response to a hurricane with extreme precipitation: a study of Hurricane Harvey in Galveston Bay, Texas. Potential Journal to submit: Journal of Marine System.

Eagles-Smith, C. A., & Ackerman, J. T. (2014). Mercury bioaccumulation in estuarine wetland fishes: Evaluating habitats and risk to coastal wildlife. ***Environmental Pollution***, 193, 147-155.

Elshanawany, R., Ibrahim, M. I., Milker, Y., Schmiedl, G., Badr, N., Kholeif, S. E., & Zonneveld, K. A. (2011). Anthropogenic impact on benthic foraminifera, Abu-Qir Bay, Alexandria, Egypt. ***Journal of Foraminiferal Research***, 41(4), 326-348.

Environmental Protection Agency (EPA) (1997). Mercury, A. I. O. A. Mercury Study Report to Congress Volume II: An Inventory of Anthropogenic Mercury Emissions in the United States.

Environmental Protection Agency (EPA), US. (1998). Mercury in solids and solutions by thermal decomposition, amalgamation, and atomic absorption spectropho-tometry. Washington, DC: Environmental Protection Agency.

FEMA, (2017). Historic Disaster Response to Hurricane Harvey in Texas. www.fema.gov/news-release/2017/09/22/historic-disaster-response-hurricane-harvey-texas

Frontalini, F., & Coccioni, R. (2008). Benthic foraminifera for heavy metal pollution monitoring: a case study from the central Adriatic Sea coast of Italy. ***Estuarine, Coastal and Shelf Science***, 76(2), 404-417.

Ganote, C. E., & Vander Heide, R. S. (1987). Cytoskeletal lesions in anoxic myocardial injury. A conventional and high-voltage electron-microscopic and immunofluorescence study. ***The American Journal of Pathology***, 129(2), 327.

Geslin, E., Debenay, J. P., & Lesourd, M. (1998). Abnormal wall textures and test deformation in Ammonia (hyaline foraminifer). ***Journal of Foraminiferal Research***, 28(2), 148-156.

Geslin, E., Debenay, J. P., Duleba, W., & Bonetti, C. (2002). Morphological abnormalities of foraminiferal tests in Brazilian environments: comparison between polluted and non-polluted areas. ***Marine Micropaleontology***, 45(2), 151-168.

Hald, M., & Steinsund, P. I. (1992). Distribution of surface sediment benthic foraminifera in the southwestern Barents Sea. ***Journal of Foraminiferal Research***, 22(4), 347-362.

Haynes, J.R., (1981). Foraminifera. John Wiley & Sons, New York, 433 pp.

Heiri, O., Lotter, A. F., & Lemcke, G. (2001). Loss on ignition as a method for estimating organic and carbonate content in sediments: reproducibility and comparability of results. ***Journal of Paleolimnology***, 25(1), 101-110.

van Hengstum, P. J., Scott, D. B., Gröcke, D. R., & Charette, M. A. (2011). Sea level controls sedimentation and environments in coastal caves and sinkholes. ***Marine Geology***, 286(1-4), 35-50.

Howell, N. L., Rifai, H. S., & Koenig, L. (2011). Comparative distribution, sourcing, and chemical behavior of PCDD/Fs and PCBs in an estuary environment. Chemosphere, 83(6), 873-881.

Jayaraju, N., Reddy, B. S. R., & Reddy, K. R. (2011). Anthropogenic impact on Andaman coast monitoring with benthic foraminifera, Andaman Sea, India. ***Environmental Earth Sciences***, 62(4), 821-829.

Kennish, M. J. (1992). Ecology of Estuaries. Anthropogenic effects. CRC. Press. Inc., Boca Raton F, 1.

Kennish, M. J. (2002). Environmental threats and environmental future of estuaries. ***Environmental conservation***, *29*(1), 78-107.

Knap, A., Turner, N. R., Bera, G., Abigail Renegar, D., Frank, T., Sericano, J., & Riegl, B. M. (2017). SHORT-TERM TOXICITY OF 1-METHYLNAPHTHALENE TO AMERICAMYSIS BAHIA AND FIVE DEEP-SEA CRUSTACEANS. Environmental toxicology and chemistry.

Kramer, K. J., & Botterweg, J. (1991). Aquatic biological early warning systems: an overview. Bioindicators and environmental management, 95-126.

Le Cadre, V., & Debenay, J. P. (2006). Morphological and cytological responses of Ammonia (foraminifera) to copper contamination: Implication for the use of foraminifera as bioindicators of pollution. Environmental Pollution, 143(2), 304-317.

Lee, J.J., Anderson, O.R., (1991). Biology of Foraminifera. Academic Press, London, San Diego and New York, 368 pp.

Lester, L. J., & Gonzalez, L. A. (2015). The state of the bay: a characterization of the Galveston Bay ecosystem. Texas Commission on Environmental Quality, Galveston Bay Estuary Program, Houston, USA.

Linder, S. H., Marko, D., & Sexton, K. (2008). Cumulative cancer risk from air pollution in Houston: disparities in risk burden and social disadvantage. 4312-4322

Linke, P., & Lutze, G. F. (1993). Microhabitat preferences of benthic foraminifera—a static concept or a dynamic adaptation to optimize food acquisition?. ***Marine Micropaleontology***, 20(3-4), 215-234.

Liu, G., Cai, Y., & O'Driscoll, N. (Eds.). (2011). ***Environmental chemistry and toxicology of mercury***. John Wiley & Sons.

Mackensen, A., Sejrup, H. P., & Jansen, E. (1985). The distribution of living benthic foraminifera on the continental slope and rise off southwest Norway. ***Marine Micropaleontology***, 9(4), 275-306.

Martínez-Colón, M., Hallock, P., & Green-Ruíz, C. (2009). Strategies for using shallow-water benthic foraminifers as bioindicators of potentially toxic elements: a review. ***Journal of Foraminiferal Research***, 39(4), 278-299.

Mastersizer 2000. (n.d.). Retrieved February 20, 2015, from http://www.malvern.com/en/products/product-range/mastersizer-range/mastersizer-2000/

Morse, J. W., Presley, B. J., Taylor, R. J., Benoit, G., & Santschi, P. (1993). Trace metal chemistry of Galveston Bay: water, sediments and biota. ***Marine Environmental Research***, *36*(1), 1-37.

Morvan, J., Debenay, J. P., Jorissen, F., Redois, F., Bénéteau, E., Delplancke, M., & Amato, A. S. (2006). Patchiness and life cycle of intertidal foraminifera:

implication for environmental and paleoenvironmental interpretation. ***Marine Micropaleontology***, 61(1), 131-154.

Mumtaz, M., & George, J. (1995). Toxicological profile for polycyclic aromatic hydrocarbons (PAHs). US Department of Human and Health Services. Agency for Toxic Substances and Disease Registry, Atlanta, GA.

Murray, J. W. (1991). Ecology and Palaeoecology of Benthic Foraminifera. Longman, Harlow.

Murray, J. W. (2006). Ecology and applications of benthic foraminifera. ***Cambridge University Press***.

Murray, J. W., & Alve, E. (2002). Benthic foraminifera as indicators of environmental change: ***Estuaries, Shelf and Upper Slope***.

Nichols, M. M. (1989). Sediment accumulation rates and relative sea-concentration rise in lagoons. ***Marine geology***, *88*(3-4), 201-219.

Nittrouer, C. A., Sternberg, R. W., Carpenter, R., & Bennett, J. T. (1979). The use of Pb-210 geochronology as a sedimentological tool: application to the Washington continental shelf. Marine Geology, 31(3-4), 297-316.

van Oldenborgh, G. J., van der Wiel, K., Sebastian, A., Singh, R., Arrighi, J., Otto, F., ... & Cullen, H. (2017). Attribution of extreme rainfall from Hurricane Harvey, August 2017. ***Environmental Research Letters***, *12*(12), 124009.

Poag, C. W. (2015). Benthic Foraminifera of the Gulf of Mexico: Distribution, ecology, paleoecology. Texas A&M University Press.

Polyak, L., Korsun, S., Febo, L. A., Stanovoy, V., Khusid, T., Hald, M., & Lubinski, D. J. (2002). Benthic foraminiferal assemblages from the southern Kara Sea, a river-influenced Arctic marine environment. ***Journal of Foraminiferal Research***, 32(3), 252-273.

Ravens, T. M., Thomas, R. C., Roberts, K. A., & Santschi, P. H. (2009). Causes of salt marsh erosion in Galveston Bay, Texas. ***Journal of Coastal Research***, 265-272.

Ravichandran, M., Baskaran, M., Santschi, P. H., & Bianchi, T. S. (1995). History of trace metal pollution in Sabine-Neches estuary, Beaumont, Texas. ***Environmental science & technology***, *29*(6), 1495-1503.

Resig, J. M. (1960). Foraminiferal ecology around ocean outfalls off southern California. Disposal in the Marine Environment: Pergamon Press, London, 104-121.

Roth, D. (2010). Texas Hurricane History. National Weather Service, Camp Springs, MD, 17.

Samir, A. M. (2000). The response of benthic foraminifera and ostracods to various pollution sources: a study from two lagoons in Egypt. ***Journal of Foraminiferal Research***, 30(2), 83-98.

Samir, A. M., & El-Din, A. B. (2001). Benthic foraminiferal assemblages and morphological abnormalities as pollution proxies in two Egyptian bays. ***Marine Micropaleontology***, 41(3), 193-227.

Santschi, P. H., Allison, M. A., Asbill, S., Perlet, A. B., Cappellino, S., Dobbs, C., & McShea, L. (1999). Sediment transport and Hg recovery in Lavaca Bay, as evaluated from radionuclide and Hg distributions. ***Environmental science & technology***, *33*(3), 378-391.

Santschi PH, Presley BJ, Wade TL, Garcia-Romero B, Baskaran M (2001). Historical contamination of PAHs, PCBs, DDTs, and heavy metals in Mississippi River Delta, Galveston Bay and Tampa Bay sediment cores. Marine Environmental Research 52: 51-79.

Sharma, P., Gardner, L. R., Moore, W. S., & Bollinger, M. S. (1987). Sedimentation and bioturbation in a salt marsh as revealed by 210Pb, 137Cs, and 7Be studies. Limnology and Oceanography, 32(2), 313-326.

Sen Gupta, B.K., (1999). Modern Foraminifera. Kluwer Academic Publisher, Dordrecht.

Sharifi, A. R., Croudace, I. W., & Austin, R. L. (1991). Benthic foraminiferids as pollution indicators in Southampton Water, southern England, UK. ***Journal of Micropaleontology***, 10(1), 109-113.

USGS (2002). Houston-Galveston Bay Area, Texas, From Space—A New Tool for Mapping Land Subsidence. USGS Fact Sheet 110-02.

Watkins, J. G. (1961). Foraminiferal ecology around the Orange County, California, ocean sewer outfall. ***Micropaleontology***, 199-206.

Wen, L. S., Santschi, P., Gill, G., & Paternostro, C. (1999). Estuarine trace metal distributions in Galveston Bay: importance of colloidal forms in the speciation of the dissolved phase. ***Marine Chemistry***, 63(3), 185-212.

The Weather Channel (2017). Historic Hurricane Harvey's Recap. *The Weather Channel*, *2*.

White, W. A., Tremblay, T. A., Wermund Jr, E. G., & Handley, L. R. (1993). Trends and status of wetland and aquatic habitats in the Galveston Bay system, Texas. Galveston Bay National Estuary Program.

Whitworth, K. W., Symanski, E., & Coker, A. L. (2008). Childhood lymphohematopoietic cancer incidence and hazardous air pollutants in southeast Texas, 1995–2004. ***Environmental Health Perspectives***, *116*(11), 1576.

Williams, J. R., Dellapenna, T. M., & Lee, G. H. (2013). Shifts in depositional environments as a natural response to anthropogenic alterations: Nakdong Estuary, South Korea. ***Marine Geology***, 343, 47-61.

Wollenburg, J. E., & Mackensen, A. (1998). On the vertical distribution of living (Rose Bengal stained) benthic foraminifers in the Arctic Ocean. ***Journal of Foraminiferal Research***, 28(4), 268-285.

Yanko, V., Flexer, A., (1991). Foraminiferal benthonic assemblages as indicators of pollution (an example of Northwestern shelf of the Black Sea). In: Proceedings of Third Annual Symposium on the Mediterranean Margin of

Israel, Institute Oceanography and Limnology, Haifa, Israel, Abstract Volume, 5 pp.

Yanko, V., & Kronfeld, J. (1992). Low and high magnesian calcitic tests of benthic foraminifera chemically mirror morphological deformations. In Proc. IV Int. Conf. Paleoceanogr., Kiel, Germany (Vol. 308).

Yanko, V., & Kronfeld, J. (1993). Trace metal pollution affects the carbonate chemistry of benthic foraminiferal shell. In Israel Society for Ecology and Environmental Quality Sciences, 24th Annual Meeting, Tel Aviv University (p. 46).

Yanko, V., Kronfeld, J., & Flexer, A. (1994). Response of benthic Foraminifera to various pollution sources; implications for pollution monitoring. ***Journal of Foraminiferal Research***, 24(1), 1-17.

Yanko, V., Ahmad, M., & Kaminski, M. (1998). Morphological deformities of benthic foraminiferal tests in response to pollution by heavy metals; implications for pollution monitoring. ***Journal of Foraminiferal Research***, 28(3), 177-200.

Yanko, V., Arnold, A. J., & Parker, W. C. (1999). Effects of marine pollution on benthic foraminifera. ***Modern Foraminifera***, 13, 217.

Yeager, K. M., Brinkmeyer, R., Rakocinski, C. F., Schindler, K. J., & Santschi, P. H. (2010). Impacts of dredging activities on the accumulation of dioxins in surface sediments of the Houston Ship Channel, Texas. ***Journal of Coastal Research***, 743-752.